Chapter 1

Introduction

In recent years, many scholars have devoted themselves to study the applications of the fractional order system to physics and engineering such as viscoelastic systems [1], dielectric polarization, and electromagnetic waves. More recently, there is a new trend to investigate the control [2] and dynamics [3-10] of the fractional order dynamical systems [11-14]. In [1] it has been shown that nonlinear chaotic systems can still behave chaotically when their models become fractional. In [11], chaos control was investigated for fractional chaotic systems by the ‘‘backstepping’’ method of nonlinear control design. In [12] and [13], it was found that chaos exists in a fractional order Chen system with order less than 3. Linear feedback control of chaos in this system was also studied. In [14], chaos synchronization of fractional order chaotic systems were studied. The existence and uniqueness of solutions of initial value problems for fractional order differential equations have been studied in the literature [15-18]. In this paper, chaotic behaviors of a fractional order double van der Pol system are studied by phase portraits [19-24] and Poincaré maps [25-32]. It is found that chaos exists in this system with order from 3.9 down to 0.4 much less than the number of states of the system. Linear transfer function approximations of the fractional integrator block are calculated for a set of fractional orders in [0.1, 0.9] based on frequency domain arguments [33].

Chaos synchronization is an important problem in nonlinear science. Since the discovery of chaos synchronization by Pecora and Carroll [34], there have been tremendous interests in studying the synchronization of various chaotic systems **[35–49].** Most of synchronizations can only realize when there exist various couplings between two chaotic systems. A major drawback of these approaches is that they, to some extent, require mutually coupled structures. In practice, such as in physical and electrical systems, sometimes it is difficult even impossible to couple two chaotic systems. In comparison with coupled chaotic systems, synchronization between the uncoupled chaotic systems has many advantages [50,51]. In this paper, the variable of a third double van der Pol system substituted for the strength of two corresponding mutual coupling term of two identical chaotic double van der Pol system, give rise to their complete synchronization

(CS) or anti-synchronization (AS). Numerical simulations show that either CS or AS depends on initial conditions and on the strengths of the substituting chaotic variable.

There have been tremendous interests in studying the complete synchronization (CS) and antisynchronization (AS) of various chaotic systems [52–91]. Here, we focus on the synchronization and antisynchronization of two identical double van der Pol systems whose corresponding parameters are replaced by a white noise, a Rayleigh noise respectively. It is noted that whether CS or AS appears depends on the driving strength [92-98].

Since chaos control problem was firstly considered by Ott et al. [99], it has been investigated extensively by lots of authors. Many linear and nonlinear control methods have been employed to control chaos [100-109]. Simple linear feedback control method was proposed [101]. The authors proposed time delay feedback control method to control chaotic system in [102-103]. Sliding variable method was employed to control chaos in [104-107]. Backstepping method was used to control chaotic systems in [108]. Adaptive control method was also used to control chaotic system [109-111]. However, traditional adaptive chaos control is limited for the same system. Proposed pragmatical adaptive control method enlarges the function of chaos control. We can control a chaotic system to any given simple unchaotic system or to any more complex given chaotic system [123-127]. Based on a pragmatical theorem of asymptotical stability using the concept of probability, an adaptive control law is derived such that it can be proved strictly that the zero solution of error dynamics and of parameter dynamics is asymptotically stable [128-129]. Numerical results are given for a chaotic double van der Pol system controlled to a double Duffing system and to an exponentially damped-simple harmonic system.

This thesis is organized as follows. Chapter 2 gives the dynamic equation of double van der Pol system. The fractional derivative and its approximation are introduced. The system under study is described both in its integer and fractional forms. Numerical simulation results are presented.

In Chapter 3, numerical simulations of synchronization scheme based on driving the corresponding parameters of two chaotic systems by a chaotic signal of a third system are presented. In Chapter 4, numerical simulations of chaos complete synchronization and antisynchronization by replacing two corresponding parameters of two uncoupled

identical double van der Pol chaotic dynamical systems by a white noise, a Rayleigh noise respectively.

In Chapter 5, numerical simulations for control of a chaotic double van der Pol system to a given chaotic double Duffing system and to an exponentially damped-simple harmonic system, are based on a new pragmatical adaptive control method. In Chapter 6, conclusions are drawn.

Chapter 2

Chaos in a Double Van der Pol System and in Its Fractional Order System

In this chapter, the dynamic equation of double van der Pol system is given. The fractional derivative and its approximation are introduced. The system under study is described both in its integer and fractional forms. Numerical simulation results are presented.

2.1 Fractional derivative and its approximation

Two commonly used definitions for the general fractional differintegral are the Grunwald definition and the Riemann-Liouville definition. The Riemann-Liouville definition of the fractional integral is given here as [27]

$$\frac{d^q f(t)}{dt^q} = \frac{1}{\Gamma(-q)} \int_0^t \frac{f(\tau)}{(t-\tau)^{q+1}} d\tau, q < 0 \tag{2.1}$$

where q can have noninteger values, and thus the name fractional differintegral. Notice that the definition is based on integration and more importantly is a convolution integral for $q < 0$. When $q > 0$, then the usual integer nth derivative must be taken of the fractional $(q–n)$th integral, and yields the fractional derivative of order q as

$$\frac{d^q f}{dt^q} = \frac{d^n}{dt^n}\left[\frac{d^{q-n} f}{dt^{q-n}}\right], \quad \text{q>0 and n an integer>q} \tag{2.2}$$

This appears so vastly different from the usual intuitive definition of derivative and integral that the reader must abandon the familiar concepts of slope and area and attempt to get some new insight. Fortunately, the basic engineering tool for analyzing linear systems, the Laplace transform, is still applicable and works as one would expect; that is,

$$L\left\{\frac{d^q f(t)}{dt^q}\right\} = s^q L\{f(t)\} - \sum_{k=0}^{n-1} s^k \left[\frac{d^{q-1-k} f(t)}{dt^{q-1-k}}\right]_{t=0}, \text{ for all q} \tag{2.3}$$

where n is an integer such that $n - 1 < q < n$. If the initial conditions are considered to be zero, this formula reduces to the more expected and comforting form

$$L\left\{\frac{d^q f(t)}{dt^q}\right\} = s^q L\{f(t)\} \tag{2.4}$$

An efficient method is to approximate fractional operators by using standard integer order operators. In [27], an effective algorithm is developed to approximate fractional order transfer functions. Basically, the idea is to approximate the system behavior in the frequency domain. By utilizing frequency domain techniques based on Bode diagrams, one can obtain a linear approximation of fractional order integrator, the order of which depends on the desired bandwidth and discrepancy between the actual and the approximate magnitude Bode diagrams. In Table 1 of [13], approximations for $1/s^q$ with q=0.1~0.9 in steps 0.1 are given, with errors of approximately 2dB. These approximations are used in following simulations.

2.2 A double van der Pol system and the corresponding fractional order system

Firstly, a van der Pol [130-132] oscillator driven by a periodic excitation is considered. The equation of motion can be written as:

$$\ddot{x} + \varphi x + a\dot{x}(x^2 - 1) - b\sin\omega t = 0 \tag{2.5}$$

where φ, a, b are constant parameters and $b\sin\omega t$ is an external excitation . In Eq. (2.5), the linear term stands for a conservative harmonic force which determines the intrinsic oscillation frequency. The self-sustaining mechanism which is responsible for the perpetual oscillation rests on the nonlinear term. Energy exchange with the external agent depends on the magnitude of displacement |x| and on the sign of velocity $\dot{x}$. During a complete cycle of oscillation, the energy is dissipated if displacement x(t) is large than one, and that energy is fed-in if |x| < 1. The time-dependent term stands for the external driving force with amplitude b and frequency ω.Eq. (2.5) can be rewritten as two first order equations:

$$\begin{cases} \dot{x} = y \\ \dot{y} = -\varphi x + a(1 - x^2)y + b \sin \omega t \end{cases} \tag{2.6}$$

With suitable parameters φ, a, b system (2.6) becomes a chaotic one. With two van der Pol systems

$$\dot{x} = y$$
$$\dot{y} = -x + b(1 - cx^2)y + a \sin \omega t$$
$$\dot{u} = v$$
$$\dot{v} = -u + e(1 - fu^2)v + d \sin \omega t$$

the double van der Pol system and its fractional order system studied is formed by replacing two external excitation $a \sin \omega t$ and $d \sin \omega t$ by mutual coupling terms au and dx:

$$\begin{cases} \dfrac{d^{\alpha 1}x}{dt^{\alpha 1}} = y \\ \dfrac{d^{\beta 1}y}{dt^{\beta 1}} = -x + b(1 - cx^2)y + au \\ \dfrac{d^{\alpha 2}u}{dt^{\alpha 2}} = v \\ \dfrac{d^{\beta 2}v}{dt^{\beta 2}} = -u + e(1 - fu^2)v + dx \end{cases} \tag{2.7}$$

where au, dx are mutual coupling terms, $\alpha_1, \alpha_2, \beta_1, \beta_2$ are either integer numbers or fractional numbers. System (2.7) becomes a new autonomous system which has not been studied before.

2.3 Numerical simulations

In this section, the phase portraits, Poincaré maps are studied for system (2.7) for $\alpha_1 + \alpha_2 + \beta_1 + \beta_2 \le 4$. A time step of 0.01 is used. It is found that chaos exists for following four different choices of parameters a, b, c, d, e, f:

A. $a = 0.0005,\ b = 0.0003,\ c = 0.0001,\ d = 0.5,\ e = 0.2,\ f = 0.1$

B. $a = -0.01,\ b = 0.2,\ c = 1,\ d = 0.3,\ e = 2,\ f = 1$

C. $a = 0.04,\ b = 0.2,\ c = 12,\ d = -0.3,\ e = 2,\ f = 1$

D. $a = -0.03,\ b = 0.07,\ c = 12,\ d = -1,\ e = 2,\ f = 1$

After 148 cases are tested, we find that chaos exists only in 21 cases. The results are shown in Table 1.

Table 1 Relation between orders of derivatives and existence of chaos.

Choice		A	B	C	D
Parameter / Number of order		$a=0.0005, b=0.0003$ $c=0.0001, d=0.5$ $e=0.5, f=0.1$	$a=-0.01, b=0.2$ $c=1, d=0.3$ $e=2,\ f=1$	$a=0.04, b=0.2$ $c=12, d=-0.3$ $e=2,\ f=1$	$a=-0.03, b=0.07$ $c=12, d=-1$ $e=2, f=1$
Integral order	**1,1,1,1**		**chaos**	**chaos**	**chaos**
Fractional order	**0.9,1,1,1**		**chaos**	**chaos**	
	0.9,0.9,1,1		**chaos**		
	0.1,1,1,1		**chaos**	**chaos**	**chaos**
	0.1,0.1,1,1	**chaos**	**chaos**	**chaos**	**chaos**
	0.1,0.1,0.1,1	**chaos**	**chaos**	**chaos**	**chaos**
	0.1,0.1,0.1,0.1	**chaos**	**chaos**	**chaos**	**chaos**

Other fractional order nonchaotic cases in choices A, B, C, D are listed in Table 2.

Table 2 Fractional order nonchaotic cases in four choices A, B, C, D.

0.9,0.9,0.9,1	**0.9,0.9,0.9,0.9**	**0.8,1,1,1**	**0.8,0.8,1,1**	**0.8,0.8,0.8,1**	**0.8,0.8,0.8,0.8**
0.7,1,1,1	**0.7,0.7,1,1**	**0.7,0.7,0.7,1**	**0.7,0.7,0.7,0.7**	**0.6,1,1,1**	**0.6,0.6,1,1**
0.6,0.6,0.6,1	**0.6,0.6,0.6,0.6**	**0.5,1,1,1**	**0.5,0.5,1,1**	**0.5,0.5,0.5,1**	**0.5,0.5,0.5,0.5**
0.4,1,1,1	**0.4,0.4,1,1**	**0.4,0.4,0.4,1**	**0.4,0.4,0.4,0.4**	**0.3,1,1,1**	**0.3,0.3,1,1**
0.3,0.3,0.3,1	**0.3,0.3,0.3,0.3**	**0.2,1,1,1**	**0.2,0.2,1,1**	**0.2,0.2,0.2,1**	**0.2,0.2,0.2,0.2**

In Choice A:

Case 1 Let $\alpha_1 = 0.1, \beta_1 = 0.1, \alpha_2 = 1, \beta_2 = 1$.Fig. 2.1 shows the phase portrait, Poincaré map of chaotic motion.

Case 2 Let $\alpha_1 = 0.1, \beta_1 = 0.1, \alpha_2 = 0.1, \beta_2 = 1$. Fig. 2.2 shows the phase portrait, Poincaré map of chaotic motion.

Case 3 Let $\alpha_1 = 0.1, \beta_1 = 0.1, \alpha_2 = 0.1, \beta_2 = 0.1$. Fig. 2.3 shows the phase portrait, Poincaré map of chaotic motion.

From Table 1, choice A, when all the parameters a, b, c, d, e, f in system (2.7) are positive, it is not easy to get chaotic phenomenon in the system with integral order derivatives. With reducing the derivative orders, the range of chaotic phase portraits decrease, and its shape changes from brush-like to star-like.

In Choice B:

Case 4 Let $\alpha_1 = 1, \beta_1 = 1, \alpha_2 = 1, \beta_2 = 1$. Fig. 2.4 shows the phase portrait, Poincaré map of chaotic motion.

Case 5 Let $\alpha_1 = 0.9, \beta_1 = 1, \alpha_2 = 1, \beta_2 = 1$.Fig. 2.5 shows the phase portrait, Poincaré map of chaotic motion.

Case 6 Let $\alpha_1 = 0.9, \beta_1 = 0.9, \alpha_2 = 1, \beta_2 = 1$. Fig. 2.6 shows the phase portrait, Poincaré map of chaotic motion.

Case 7 Let $\alpha_1 = 0.1, \beta_1 = 1, \alpha_2 = 1, \beta_2 = 1$. Fig. 2.7 shows the phase portrait, Poincaré map of chaotic motion.

Case 8 Let $\alpha_1 = 0.1, \beta_1 = 0.1, \alpha_2 = 1, \beta_2 = 1$. Fig. 2.8 shows the phase portrait, Poincaré map of chaotic motion.

Case 9 Let $\alpha_1 = 0.1, \beta_1 = 0.1, \alpha_2 = 0.1, \beta_2 = 1$. Fig. 2.9 shows the phase portrait, Poincaré map of chaotic motion.

Case 10 Let $\alpha_1 = 0.1, \beta_1 = 0.1, \alpha_2 = 0.1, \beta_2 = 0.1$. Fig. 2.10 shows the phase portrait, Poincaré map of chaotic motion.

With reducing the derivative order, the ranges of the chaotic phase portraits decrease greatly, and its shape changes from mouth-like to ring-like, hollow ellipse-like, and

finally solid ellipse-like.

In Choice C:

Case 11 Let $\alpha_1 = 1, \beta_1 = 1, \alpha_2 = 1, \beta_2 = 1$. Fig. 2.11 shows the phase portrait, Poincaré map of chaotic motion.

Case 12 Let $\alpha_1 = 0.9, \beta_1 = 1, \alpha_2 = 1, \beta_2 = 1$.Fig. 2.12 shows the phase portrait, Poincaré map of chaotic motion.

Case 13 Let $\alpha_1 = 0.1, \beta_1 = 1, \alpha_2 = 1, \beta_2 = 1$. Fig. 2.13 shows the phase portrait, Poincaré map of chaotic motion.

Case 14 Let $\alpha_1 = 0.1, \beta_1 = 0.1, \alpha_2 = 1, \beta_2 = 1$. Fig. 2.14 shows the phase portrait, Poincaré map of chaotic motion.

Case 15 Let $\alpha_1 = 0.1, \beta_1 = 0.1, \alpha_2 = 0.1, \beta_2 = 1$. Fig. 2.15 shows the phase portrait, Poincaré map of chaotic motion.

Case 16 Let $\alpha_1 = 0.1, \beta_1 = 0.1, \alpha_2 = 0.1, \beta_2 = 0.1$. Fig. 2.16 shows the phase portrait, Poincaré map of chaotic motion.

With reducing the derivative order, the ranges of the chaotic phase portraits decrease greatly, and its shape changes from ring-like to meshed ring-like, hollow ellipse-like, and finally thick hollow ellipse-like.

In Choice D:

Case 17 Let $\alpha_1 = 1, \beta_1 = 1, \alpha_2 = 1, \beta_2 = 1$. Fig. 2.17 shows the phase portrait, Poincaré map of chaotic motion.

Case 18 Let $\alpha_1 = 0.1, \beta_1 = 1, \alpha_2 = 1, \beta_2 = 1$. Fig. 2.18 shows the phase portrait, Poincaré map of chaotic motion.

Case 19 Let $\alpha_1 = 0.1, \beta_1 = 0.1, \alpha_2 = 1, \beta_2 = 1$. Fig. 2.19 shows the phase portrait, Poincaré map of chaotic motion.

Case 20 Let $\alpha_1 = 0.1, \beta_1 = 0.1, \alpha_2 = 0.1, \beta_2 = 1$. Fig. 2.20 shows the phase portrait, Poincaré map of chaotic motion.

Case 21 Let $\alpha_1 = 0.1, \beta_1 = 0.1, \alpha_2 = 0.1, \beta_2 = 0.1$. Fig. 2.21 shows the phase portrait, Poincaré map of chaotic motion.

With reducing the derivative order, the ranges of the chaotic phase portraits decrease

greatly, and its shape changes from ring-like to hollow ellipse-like, and finally haired ellipse-like. Chaos of fractional order systems only exists when one or more than one 0.1 order derivative appears.

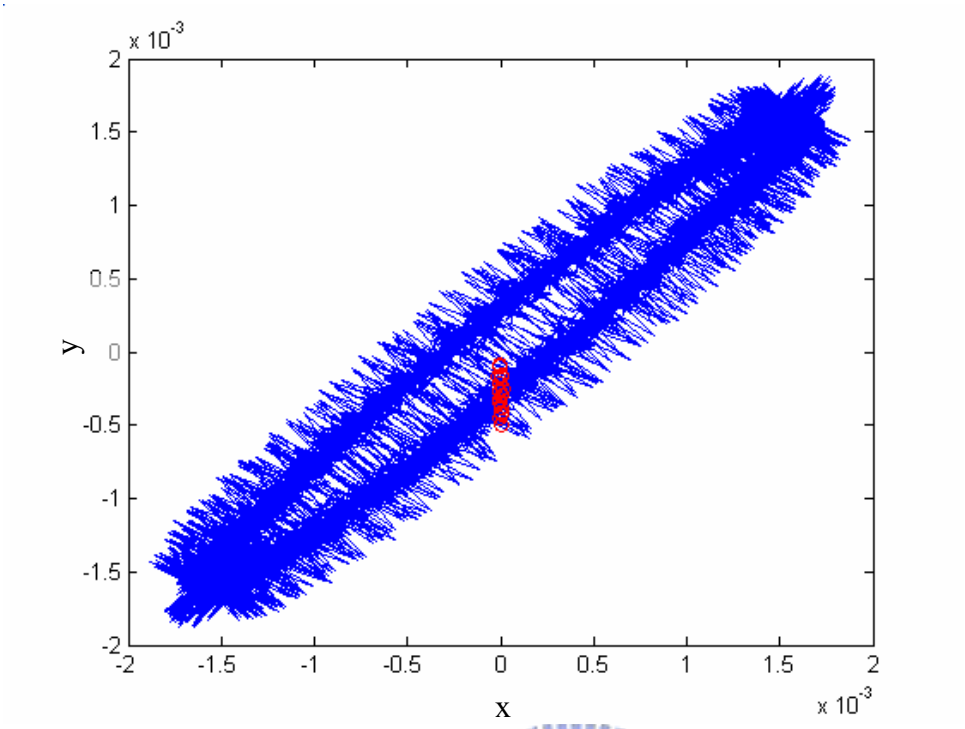

Fig 2.1: The phase portrait, Poincaré map for the fractional order double van der Pol system, $\alpha_1 = 0.1, \beta_1 = 0.1, \alpha_2 = 1, \beta_2 = 1$

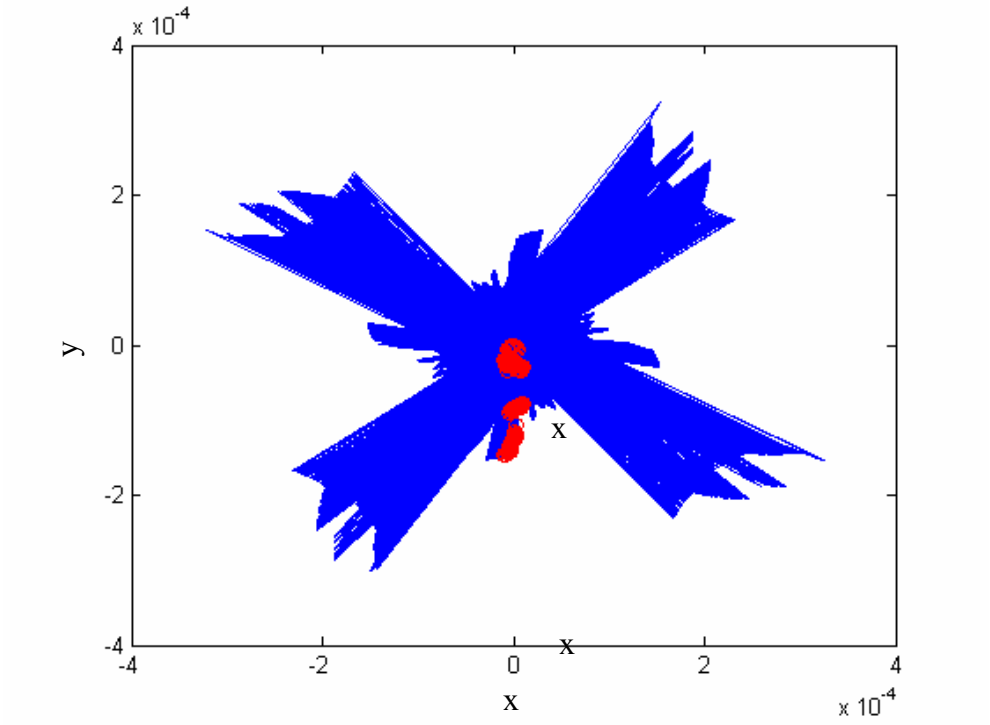

Fig 2.2: The phase portrait, Poincaré map for the fractional order double van der Pol system, $\alpha_1 = 0.1, \beta_1 = 0.1, \alpha_2 = 0.1, \beta_2 = 1$

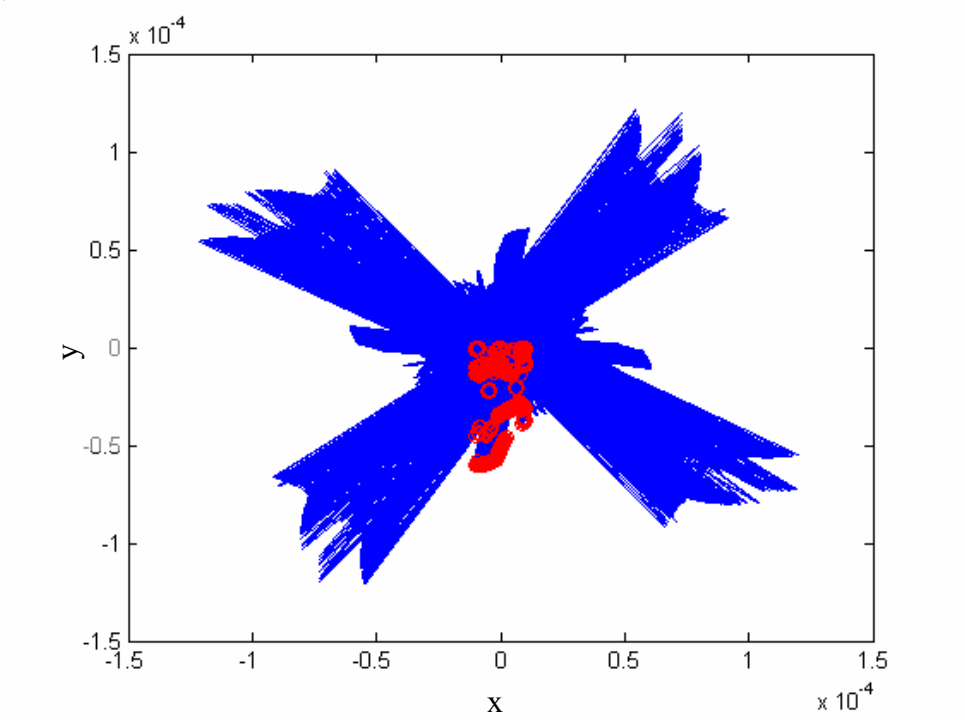

Fig 2.3: The phase portrait, Poincaré map for the fractional order double van der Pol system, $\alpha_1 = 0.1, \beta_1 = 0.1, \alpha_2 = 0.1, \beta_2 = 0.1$

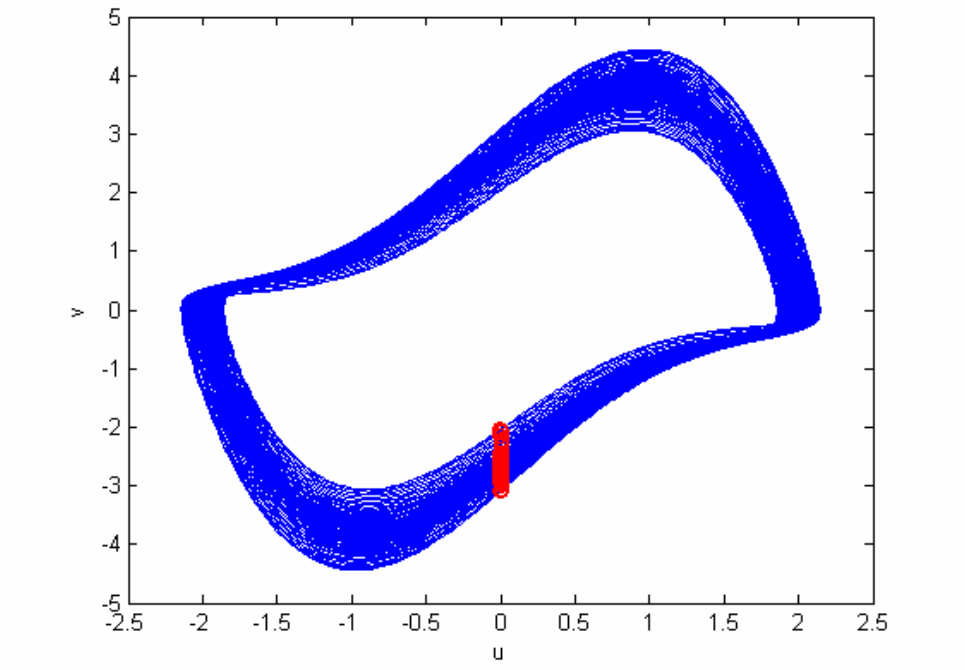

Fig 2.4: The phase portrait, Poincaré map for the fractional order double van der Pol system, $\alpha_1 = 1, \beta_1 = 1, \alpha_2 = 1, \beta_2 = 1$

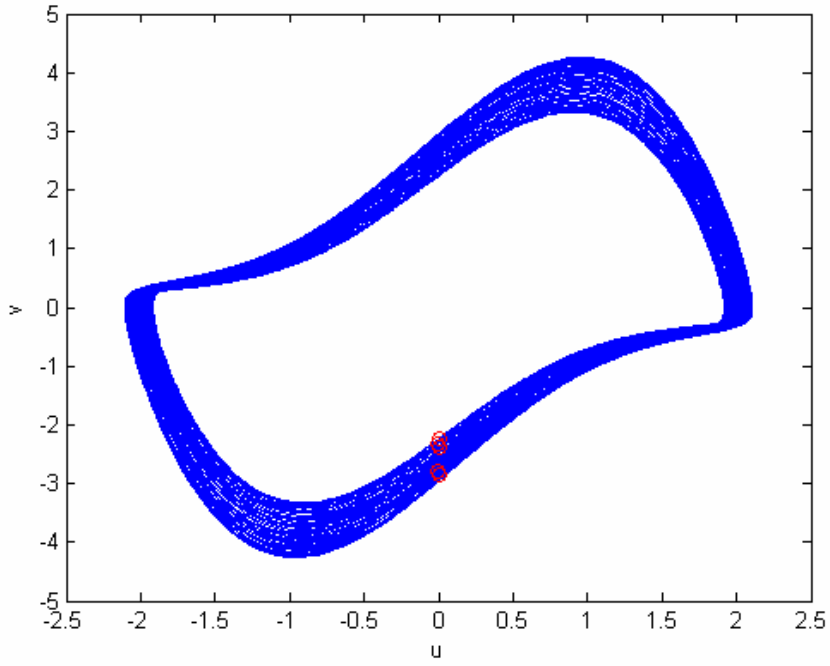

Fig 2.5: The phase portrait, Poincaré map for the fractional order double van der Pol system, $\alpha_1 = 0.9, \beta_1 = 1, \alpha_2 = 1, \beta_2 = 1$

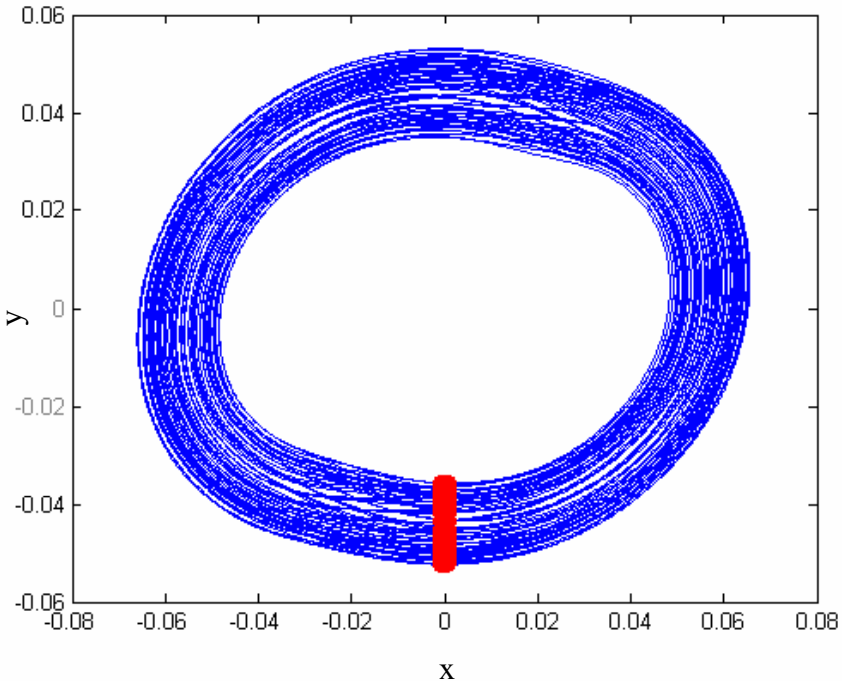

Fig 2.6: The phase portrait, Poincaré map for the fractional order double van der Pol system, $\alpha_1 = 0.9, \beta_1 = 0.9, \alpha_2 = 1, \beta_2 = 1$

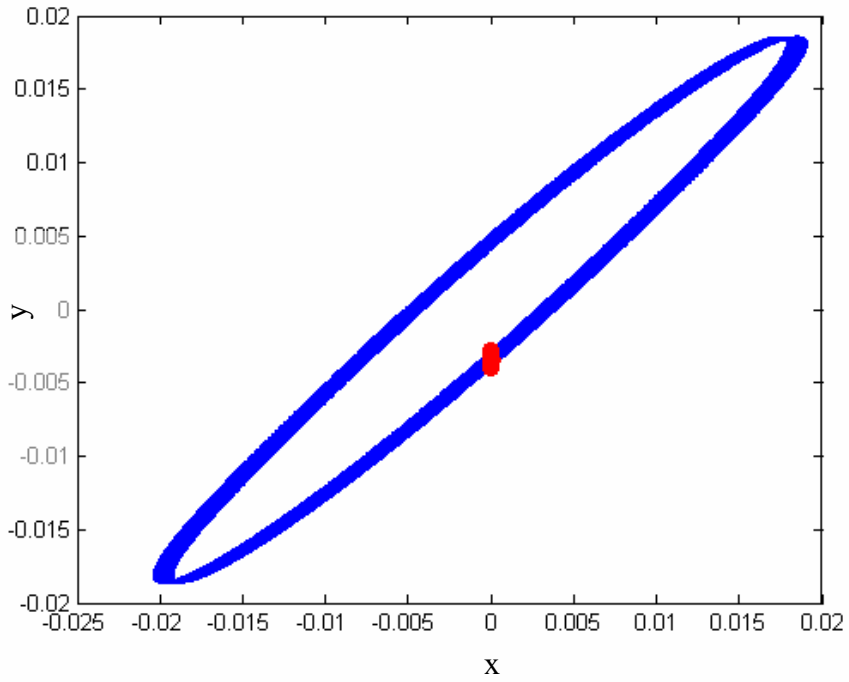

Fig 2.7: The phase portrait, Poincaré map for the fractional order double van der Pol system, $\alpha_1 = 0.1, \beta_1 = 1, \alpha_2 = 1, \beta_2 = 1$

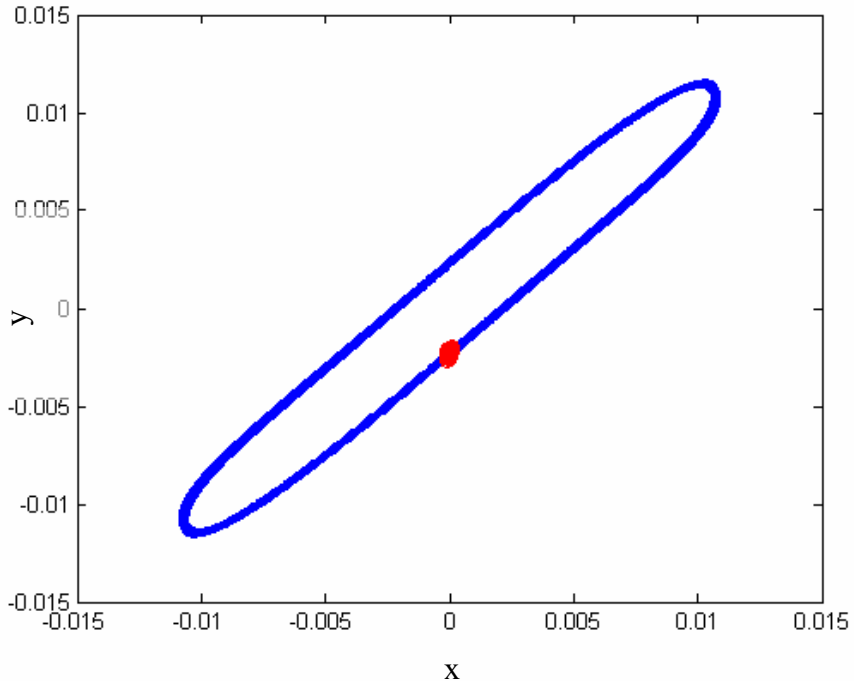

Fig 2.8: The phase portrait, Poincaré map for the fractional order double van der Pol system, $\alpha_1 = 0.1, \beta_1 = 0.1, \alpha_2 = 1, \beta_2 = 1$

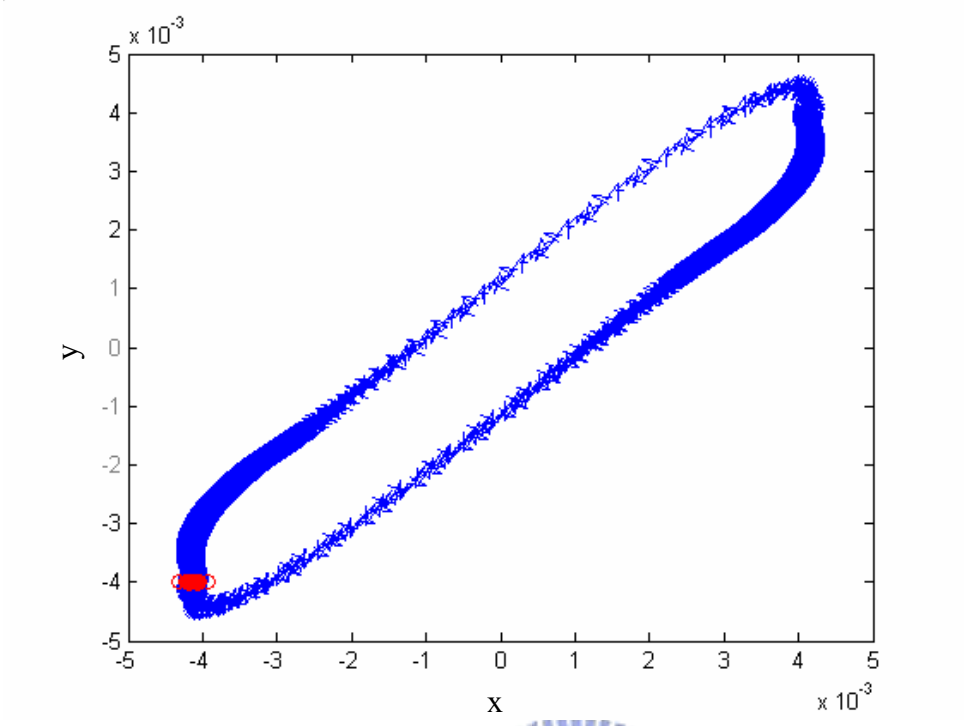

Fig 2.9: The phase portrait, Poincaré map for the fractional order double van der Pol system, $\alpha_1 = 0.1, \beta_1 = 0.1, \alpha_2 = 0.1, \beta_2 = 1$

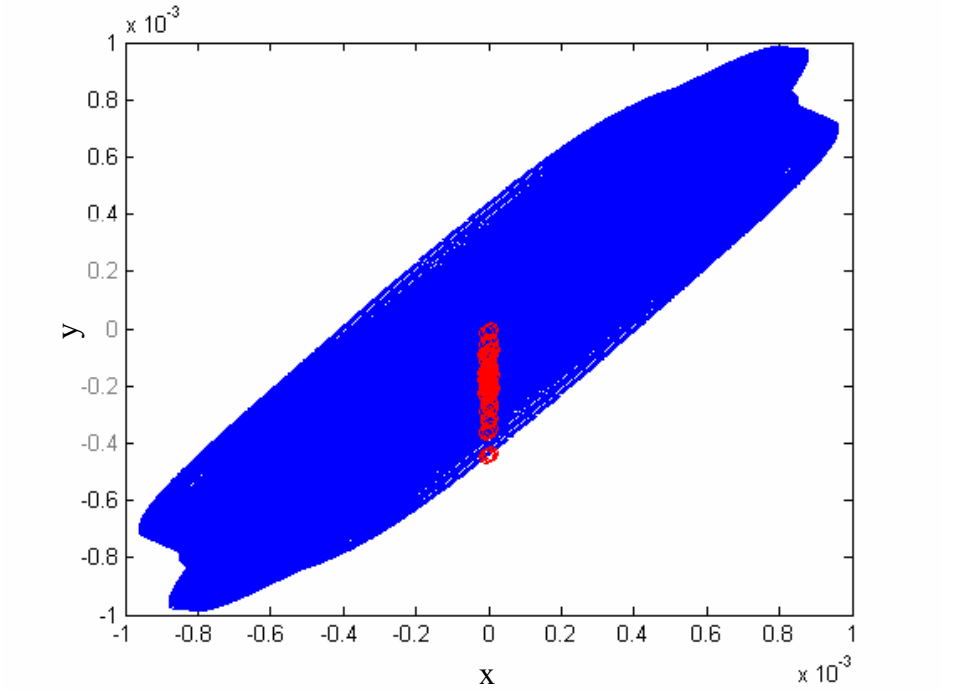

Fig 2.10: The phase portrait, Poincaré map for the fractional order double van der Pol system, $\alpha_1 = 0.1, \beta_1 = 0.1, \alpha_2 = 0.1, \beta_2 = 0.1$

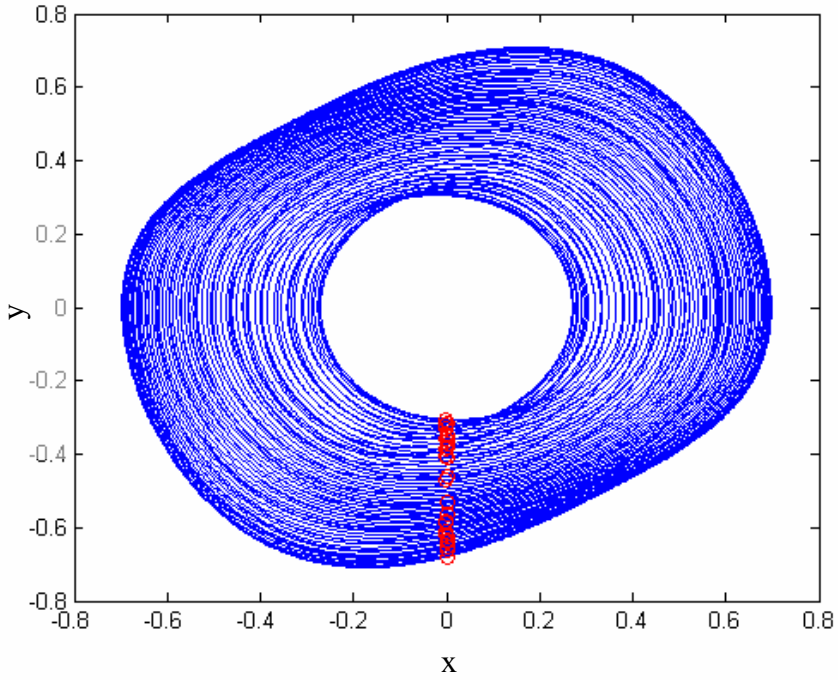

Fig 2.11: The phase portrait, Poincaré map for the fractional order double van der Pol system, $\alpha_1 = 1, \beta_1 = 1, \alpha_2 = 1, \beta_2 = 1$

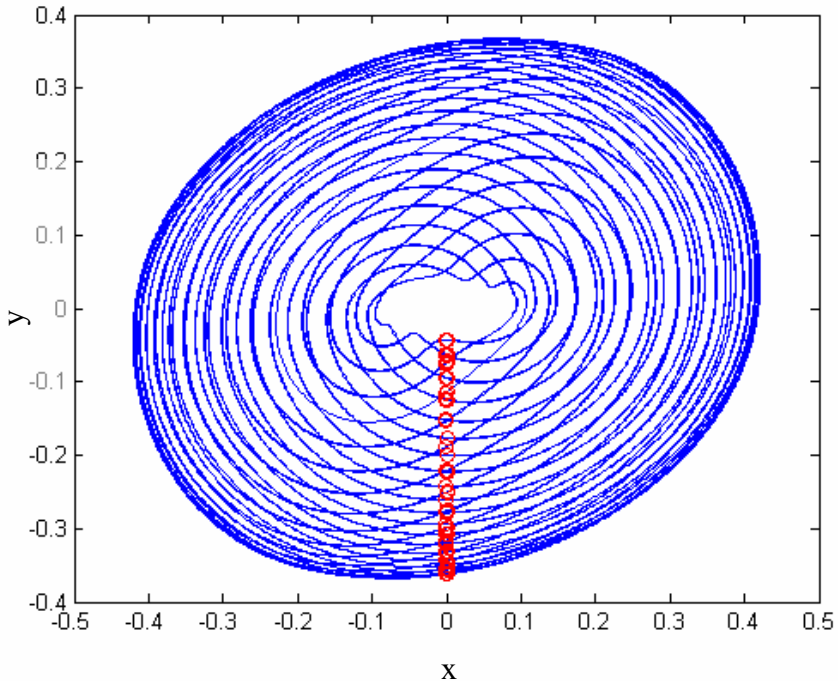

Fig 2.12: The phase portrait, Poincaré map for the fractional order double van der Pol system, $\alpha_1 = 0.9, \beta_1 = 1, \alpha_2 = 1, \beta_2 = 1$

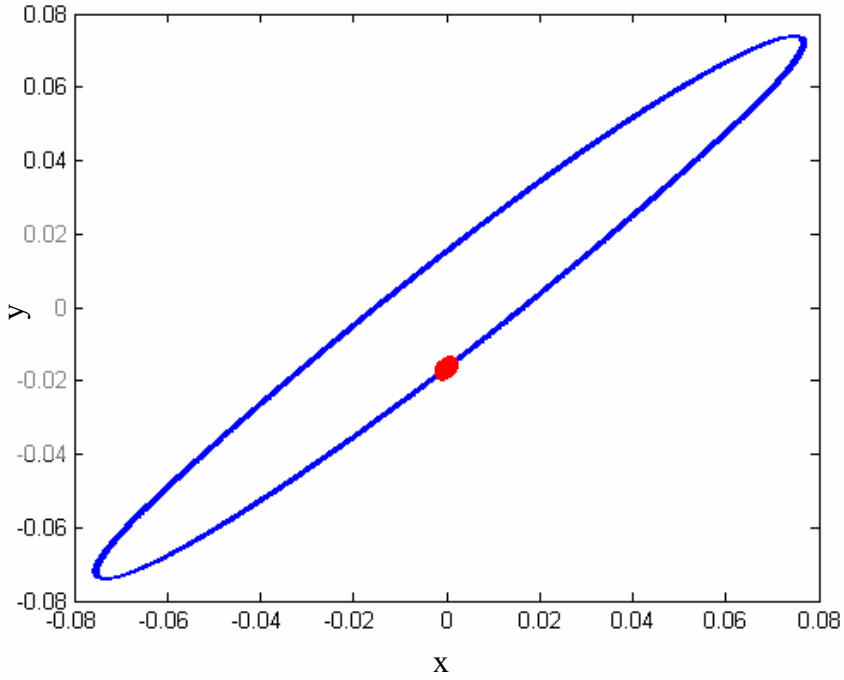

Fig 2.13: The phase portrait, Poincaré map for the fractional order double van der Pol system, $\alpha_1 = 0.1, \beta_1 = 1, \alpha_2 = 1, \beta_2 = 1$

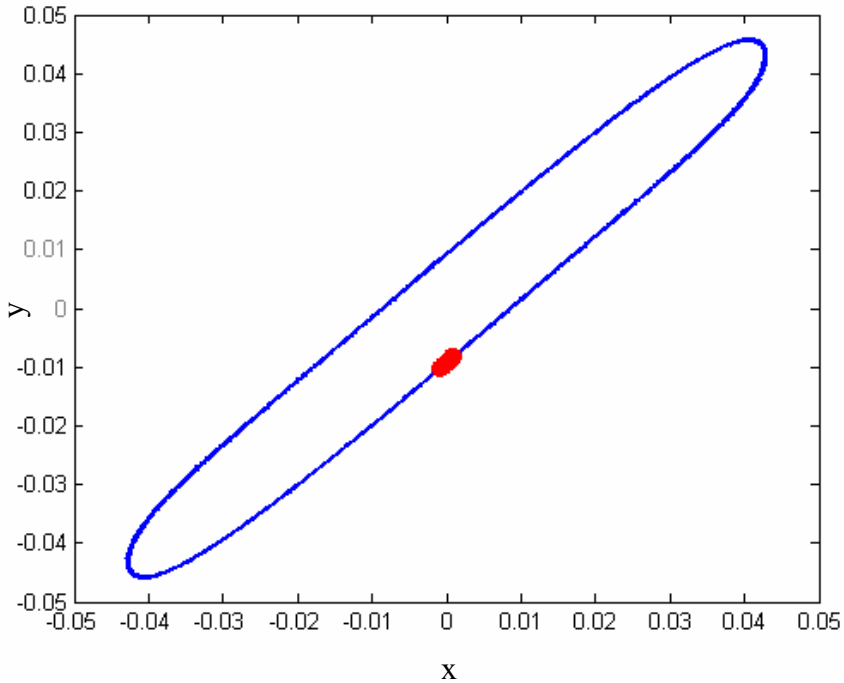

Fig 2.14: The phase portrait, Poincaré map for the fractional order double van der Pol system, $\alpha_1 = 0.1, \beta = 0.1, \alpha_2 = 1, \beta_2 = 1$

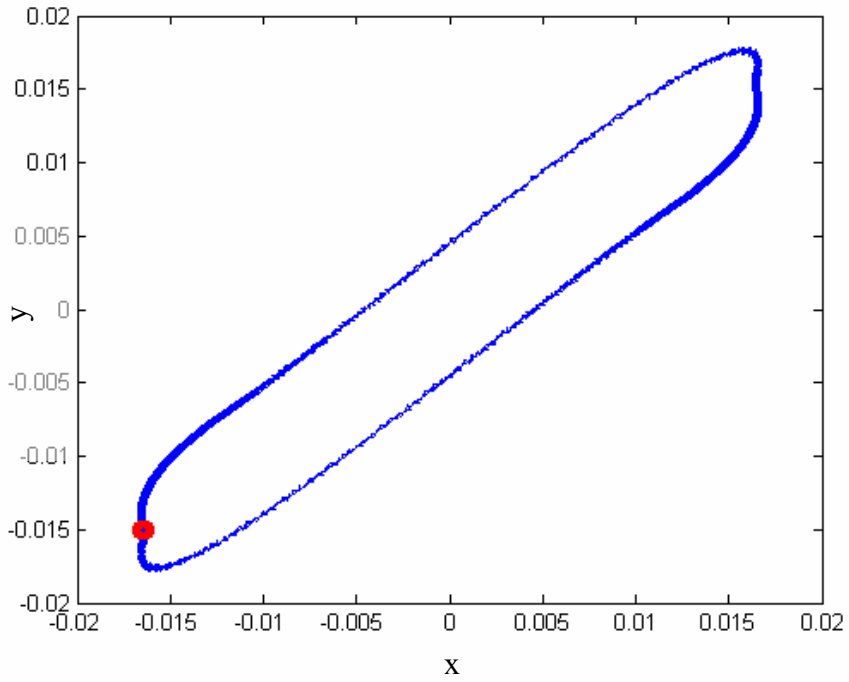

Fig 2.15: The phase portrait, Poincaré map for the fractional order double van der Pol system, $\alpha_1 = 0.1, \beta_1 = 0.1, \alpha_2 = 0.1, \beta_2 = 1$

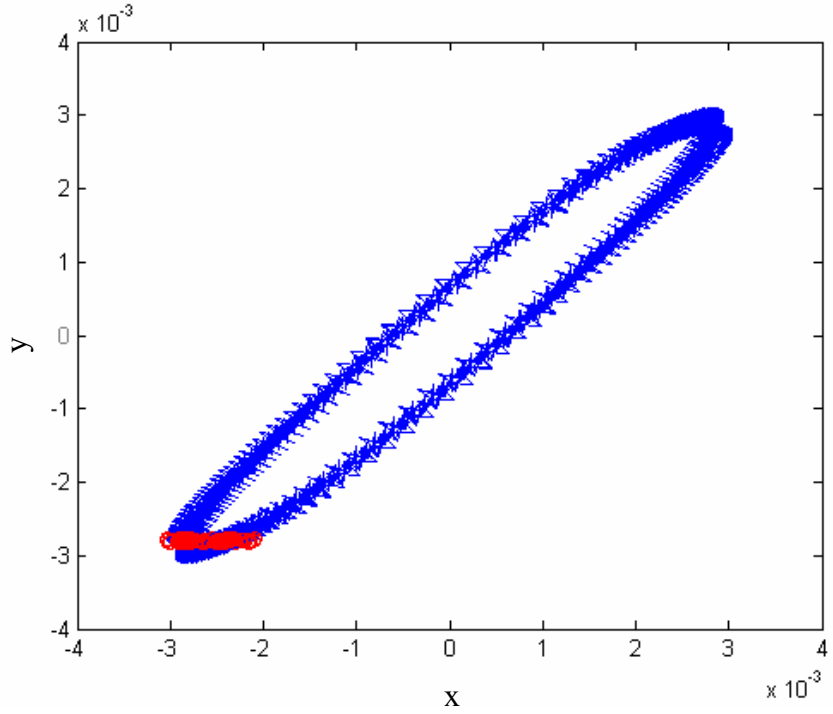

Fig 2.16: The phase portrait, Poincaré map for the fractional order double van der Pol system, $\alpha_1 = 0.1, \beta_1 = 0.1, \alpha_2 = 0.1, \beta_2 = 0.1$

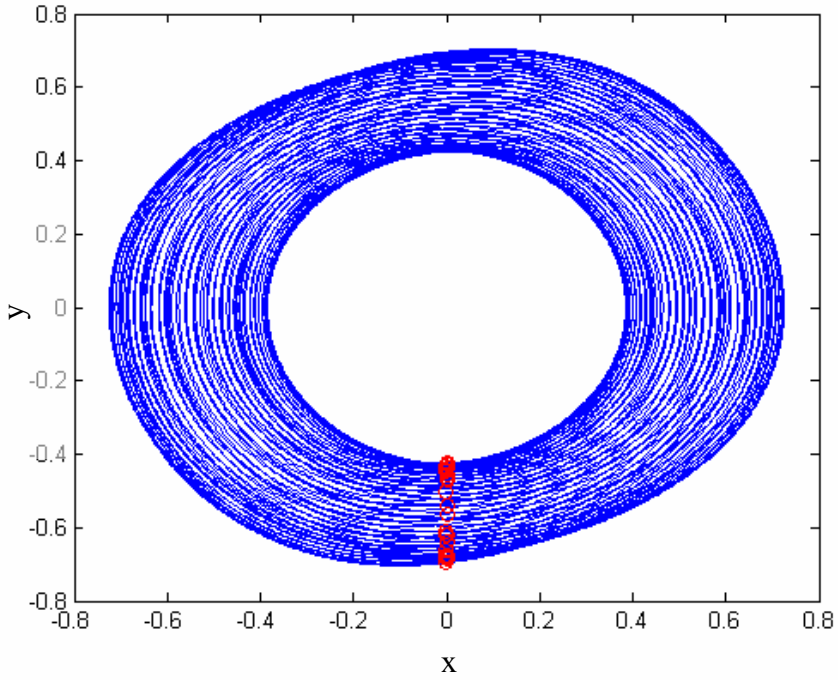

Fig 2.17: The phase portrait, Poincaré map for the fractional order double van der Pol system, $\alpha_1 = 1, \beta_1 = 1, \alpha_2 = 1, \beta_2 = 1$

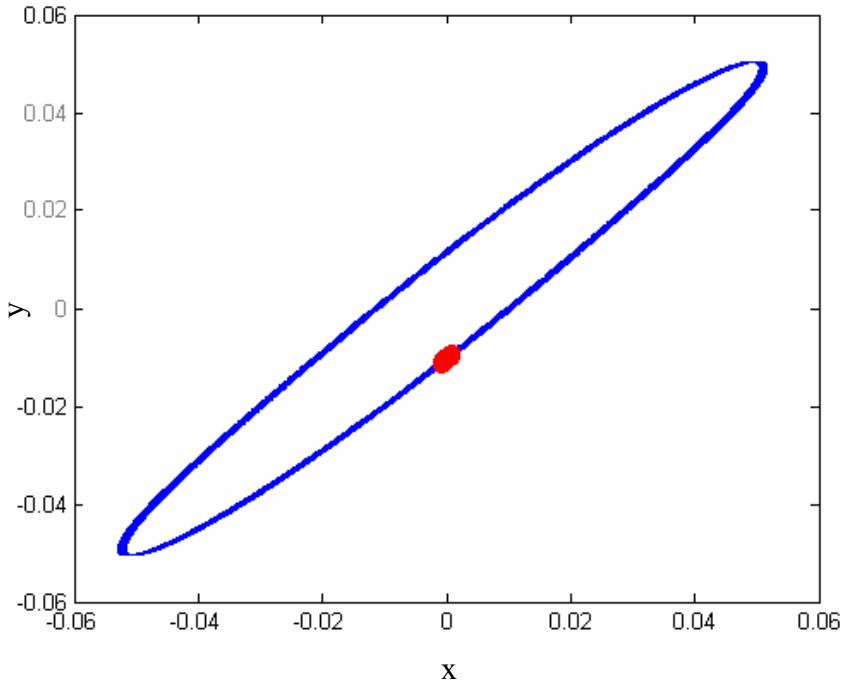

Fig 2.18: The phase portrait, Poincaré map for the fractional order double van der Pol system, $\alpha_1 = 0.1, \beta_1 = 1, \alpha_2 = 1, \beta_2 = 1$

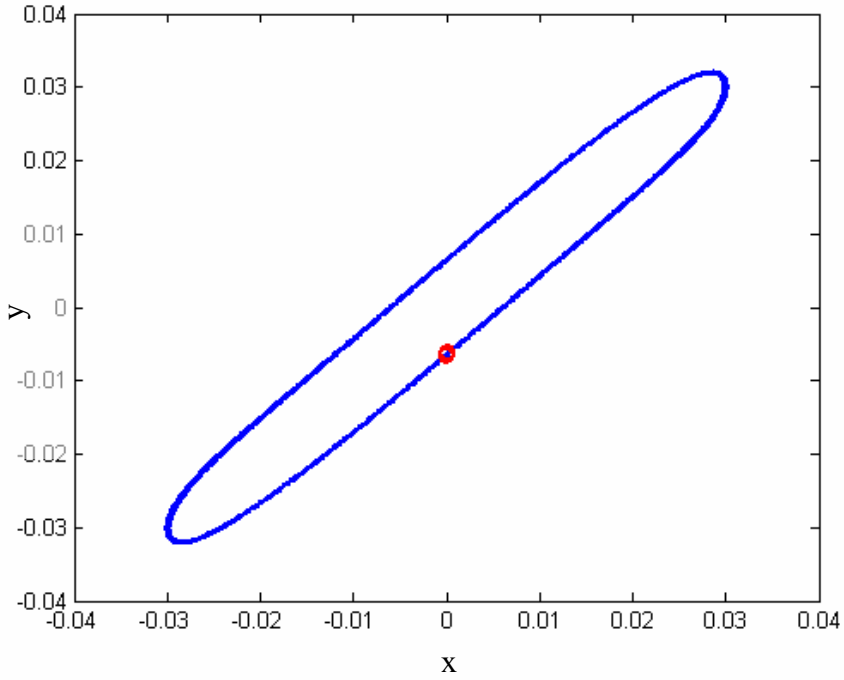

Fig 2.19: The phase portrait, Poincaré map for the fractional order double van der Pol system, $\alpha_1 = 0.1, \beta_1 = 0.1, \alpha_2 = 1, \beta_2 = 1$

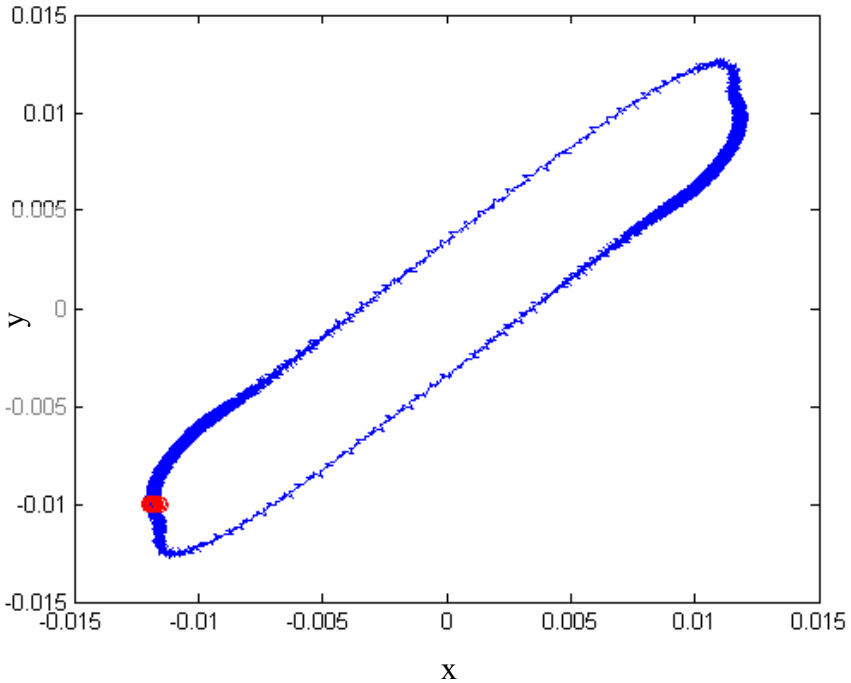

Fig 2.20: The phase portrait, Poincaré map for the fractional order double van der Pol system, $\alpha = 0.1, \beta_1 = 0.1, \alpha_2 = 0.1, \beta_2 = 1$

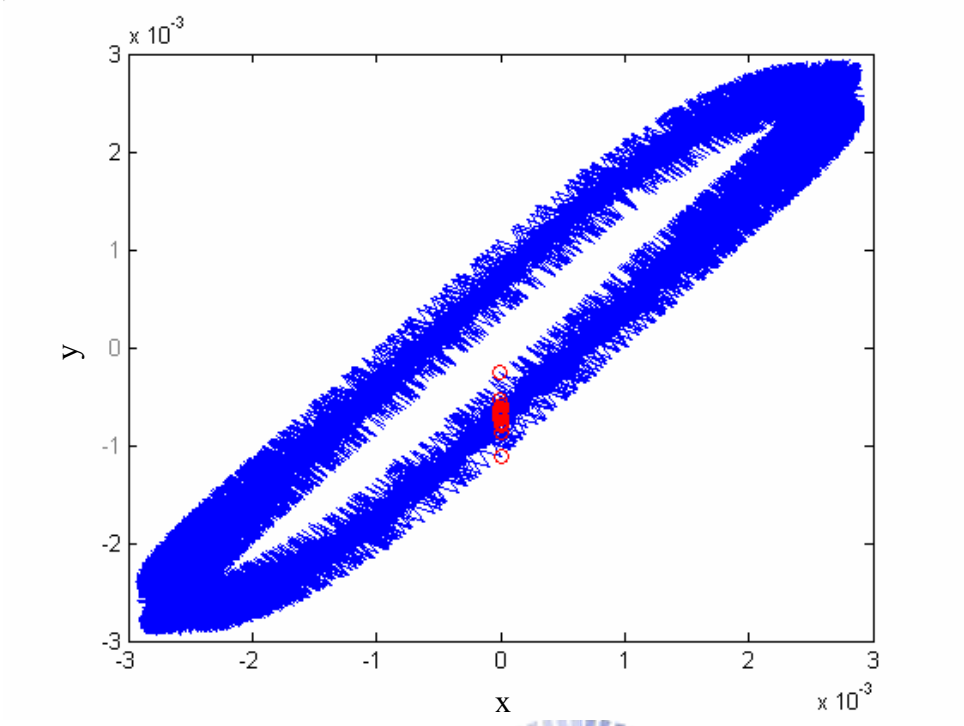

Fig 2.21: The phase portrait, Poincaré map for the fractional order double van der Pol system, $\alpha_1 = 0.1, \beta_1 = 0.1, \alpha_2 = 0.1, \beta_2 = 0.1$

Chapter 3

Chaos-excited Synchronization of Uncopuled Double Van der Pol systems

3.1 Preliminaries

Chaos synchronizations of two uncoupled identical double van der Pol systems are studied, the variable with adjustable strength of a third double van der Pol system substituted for the strength of two corresponding mutual coupling terms of two identical chaotic double van der Pol system, gives rise to their synchronization or anti-synchronization. The method is named parameter excited chaos synchronization.

3.2 Numerical simulations for synchronization between uncoupled double van der Pol system

The double van der Pol system studied in this paper consists of two van der Pol systems with mutual coupling terms instead of two external excitations:

$$\begin{cases} \dfrac{dx_1}{dt} = y_1 \\ \dfrac{dy_1}{dt} = -x_1 + b(1 - cx_1^2)y_1 + au_1 \\ \dfrac{du_1}{dt} = v_1 \\ \dfrac{dv_1}{dt} = -u_1 + e(1 - fu_1^2)v_1 + dx_1 \end{cases} \tag{3.1}$$

where au_1, dx_1 are mutual coupling terms. When a = 0.04 , b = 0.2, c = 12 , d = -0.3, e = 2, f = 1, chaos of the system are illustrated by Lyapunov exponent diagram (Fig. 3.1) and phase portrait (Fig. 3.2).

Take system (3.1) as master system, the slave system is

$$\begin{cases} \dfrac{dx_2}{dt} = y_2 \\ \dfrac{dy_2}{dt} = -x_2 + b(1 - cx_2^2)y_2 + au_2 \\ \dfrac{du_2}{dt} = v_2 \\ \dfrac{dv_2}{dt} = -u_2 + e(1 - fu_2^2)v_2 + dx_2 \end{cases} \tag{3.2}$$

A third double van der Pol system is given:

$$\begin{cases} \dfrac{dx_3}{dt} = y_3 \\ \dfrac{dy_3}{dt} = -x_3 + b(1 - cx_3^2)y_3 + au_3 \\ \dfrac{du_3}{dt} = v_3 \\ \dfrac{dv_3}{dt} = -u_3 + e(1 - fu_3^2)v_3 + dx_3 \end{cases} \tag{3.3}$$

Substituting kx_3 or ky_3 for both *a* in system (3.1) and system (3.2), respectively. and giving suitable values for k and initial conditions, we obtain that two system (3.1) and system (3.2) are either synchronized or anti-synchronized.

Matlab method is used to all of the simulations with time step 0.01. The parameters of two systems (3.1) and system (3.2) are given as a = 0.04, b = 0.2, c = 12, d = -0.3, **e** = 2, f = 1 to ensure the chaotic behavior. To verify CS and AS, it is convenient to introduce the following coordinate transformation: $E_1 = (x_1 + x_2)$ and $e_1 = (x_1 - x_2)$ and the same transformation for *y, u* and v variables. Therefore, the new coordinate systems (E_1, E_2, E_3, E_4) and (e_1, e_2, e_3, e_4) represent the sum and difference motions of the original coordinate system, respectively. We can easily see that the (e_1, e_2, e_3, e_4) subspace represents the CS case, and the (E_1, E_2, E_3, E_4) subspace for the AS one.

Choice A

Take kx_3 instead of both *a* in system (3.1) and system (3.2),and take (x_1, y_1, u_1, v_1) = (3, 4, 3, 4), (x_2, y_2, u_2, v_2) = (-3, 4, -3, 4) as the initial conditions of system (3.1) and system (3.2). For Fig. 3.3, k = 1 and for Fig. 3.4, k = 0.9. Fig. 3.3 and Fig. 3.4 show the time-series of AS (case (a)) and CS (case (b)) phenomena for different k, respectively. These simulation results indicate that the final state develops to CS or AS, depending sensitively on k in spite of the identical initial conditions in both cases.

For Fig. 3.3, e_4 (CS), E_2 (AS), E_3 (AS), converge to zero, while the other coordinates remain chaotic. For Fig. 3.4 , on the other hand, only E_2 (AS) converge to zero.

Depending on the initial conditions both AS and CS can also be observed. To study how these phenomena depend upon the initial conditions, we change the initial conditions for fixed k. The results are shown in Figs. 3.5 and 3.6. Fig. 3.5 (a) shows that the differences $e_2 = y_1 - y_2$ and $e_3=u_1 - u_2$ tend to zero. In Fig. 3.5 (b), the sum $E_4=v_1 + v_2$ tends to zero. Comparing Fig. 3.3 with Fig. 3.5, one can find that they have different behaviors. The only reason lies in the different initial conditions. Similar result also exists by comparing Fig. 3.4 with Fig. 3.6. But we have not observed the intermittent synchronization and antisynchronization states as declared in Ref. [133].

The simulation results are shown in Fig. 3.7 for different value of k. The solid circle "●" and triangle "▲" correspond to CS where parameter values k leads to synchronized behavior. While white circle "○" and triangle "△" indicate AS. The blank space means no AS or CS. We can see that the system (3.1) and system (3.2) tend to either AS or CS by using combination of different value of k and initial values. However, as we can see from Fig. 3.7, both cases agree well with the fact that the system goes to either synchronized state or anti-synchronized state depending on initial values and on k. When k = 0.8 ~ 0.82, neither synchronization nor anti-synchronization is found.

Choice B

Take kx_3 instead of both a in system (3.1) and system (3.2), and take (x_1, y_1, u_1, v_1) = (3, 4, 3, 4), (x_2, y_2, u_2, v_2) = (-3, 4, 3, 4) as the initial conditions of system (3.1) and system (3.2). For Fig. 3.8, k = 0.97 and for Fig. 3.9, k = 1.02. Fig. 3.8 and Fig. 3.9 show the time-series of AS (case (c)) and CS (case (d)) phenomena for different k, respectively. These simulation results indicate that the final state develops to CS or AS, depending sensitively on k in spite of the identical initial conditions in both cases. For Fig. 3.8, e_2 (CS) , e_3 (CS), E_4 (AS), converge to zero, while the other coordinates remain chaotic. For the Fig. 3.9 , on the other hand, e_2 (CS) , e_3 (CS), E_4 (AS) also converge to zero.

Depending on the initial conditions, both AS and CS can also be observed. To study how these phenomena depend upon the initial conditions, we change the initial conditions for fixed k. The results are shown in Figs. 3.10 and 3.11. Fig. 3.10 (a) shows that the difference $e_4=v_1 - v_2$ tends to zero. In Fig. 3.10 (b), the sums

$E_2=y_1+y_2$, $E_3=u_1+u_2$ tend to zero. Comparing Fig. 3.8 with Fig. 3.10 one can find that they have different behaviors. The only reason lies in the different initial conditions. Similar result also exists by comparing Fig. 3.9 with Fig. 3.11. But we have not observed the intermittent synchronization and antisynchronization states as declared in Ref. [133]..

The simulation results are shown in Fig. 3.12 for different value of k. The solid circle "●" and triangle "▲" correspond to CS where parameter values k leads to synchronized behavior. While white circle "○" and triangle "△" indicate AS. The blank space means no AS or CS. We can see that the system (3.1) and system (3.2) tend to either AS or CS by using combination of different value of k and initial values. However, as we can see from Fig. 3.12, both cases agree well with the fact that the system goes to either synchronized state or anti-synchronized state depending on initial values and on k. When k = 0.9 ~ 0.96 and 1.04 ~ 1.10, neither synchronization nor anti-synchronization is found.

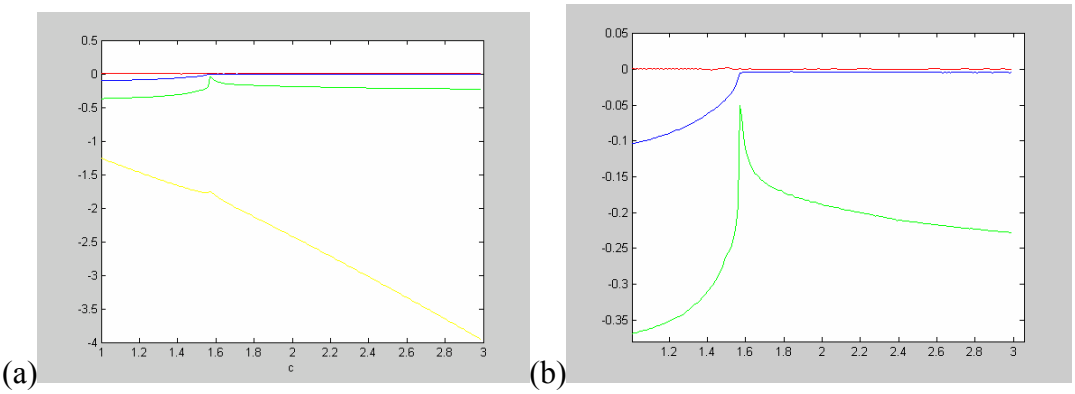

Fig. 3.1 Lyapunov exponent diagram of the double van der Pol system for c between 1.0 and 3.0 in (a) and enlarge in (b).

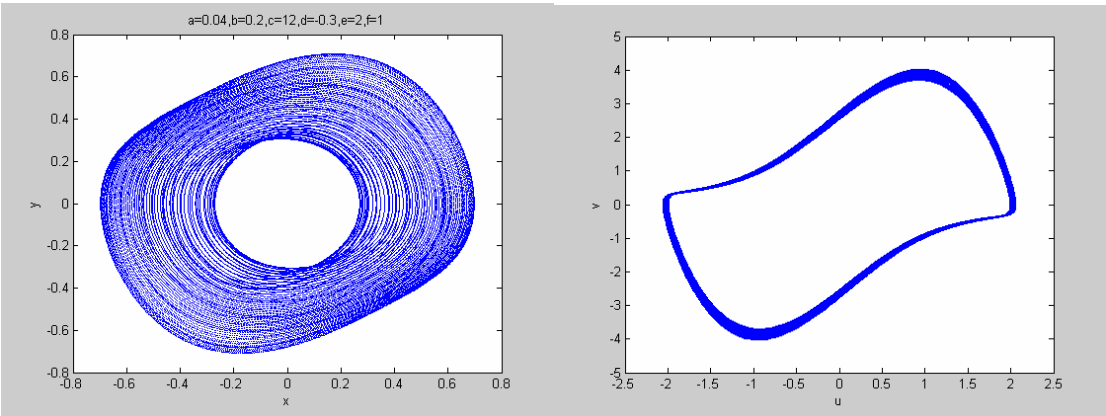

Fig. 3.2 Phase portraits of the double van der Pol system

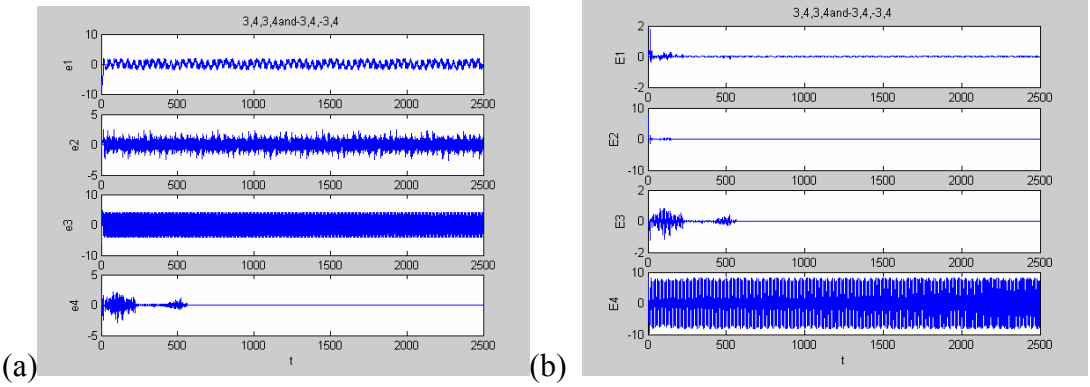

Fig. 3.3 CS and AS for initial condition(x_2, y_2, u_2, v_2)= (-3, 4, -3, 4) and k=1, (a) e_1, e_2, e_3, e_4 (b) E_1, E_2, E_3, E_4.

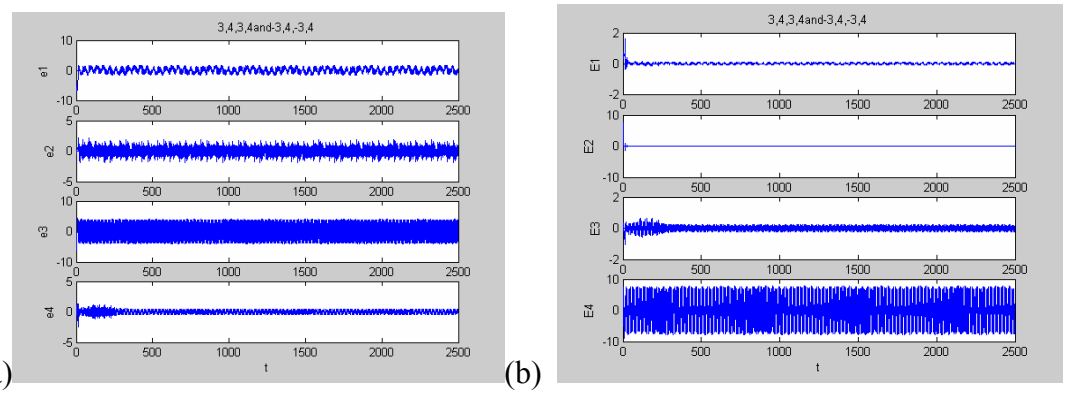

(a) (b)

Fig. 3.4 AS for initial condition $(x_2, y_2, u_2, v_2) = (-3, 4, -3, 4)$ and k=0.9,
(a) e_1, e_2, e_3, e_4 (b) E_1, E_2, E_3, E_4.

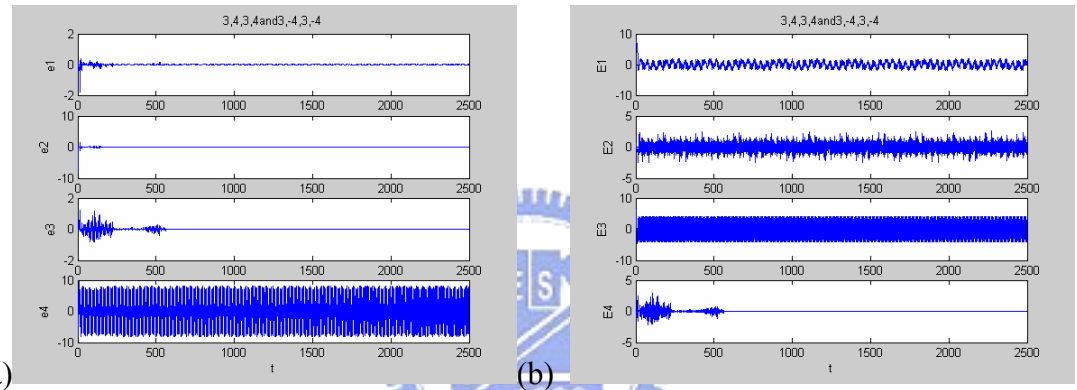

(a) (b)

Fig. 3.5 CS and AS for initial condition $(x_2, y_2, u_2, v_2) = (3, -4, 3, -4)$ and k=1,
(a) e_1, e_2, e_3, e_4 (b) E_1, E_2, E_3, E_4.

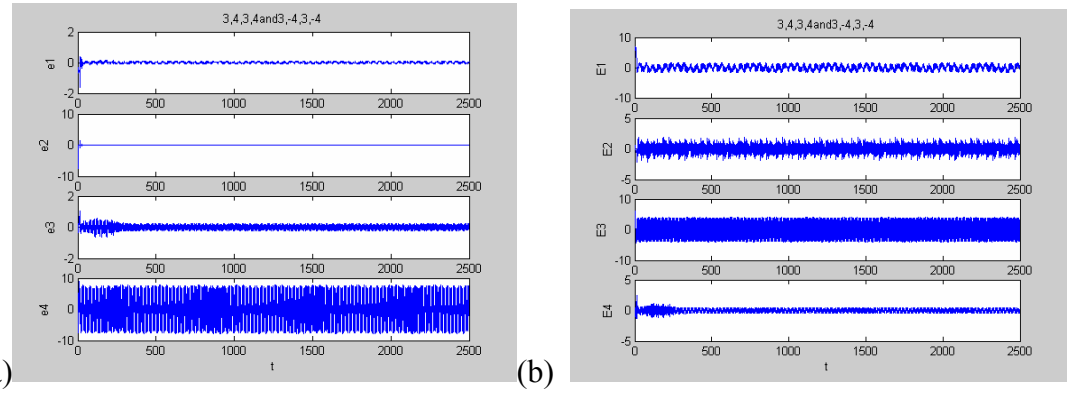

(a) (b)

Fig. 3.6 CS for initial condition$(x_2, y_2, u_2, v_2) = (3, -4, 3, -4)$ and k=0.9,
(a) e_1, e_2, e_3, e_4 (b) E_1, E_2, E_3, E_4.

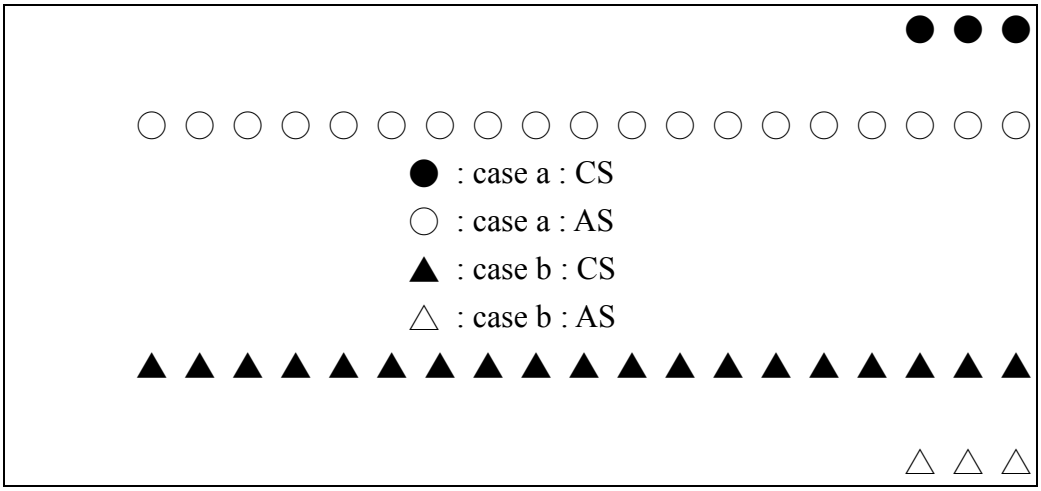

0.8 0.81 0.82 0.83 0.84 0.85 0.86 0.87 0.88 0.89 0.90 0.91 0.92 0.93 0.94 0.95 0.96 0.97 0.98 0.99 1.0 1.01

k

Fig. 3.7 CS or AS vs. the k for different initial conditions,
case a: $(x_1, y_1, u_1, v_1) = (3, 4, 3, 4)$ and $(x_2, y_2, u_2, v_2) = (-3, 4, -3, 4)$
case b: $(x_1, y_1, u_1, v_1) = (3, 4, 3, 4)$ and $(x_2, y_2, u_2, v_2) = (3, -4, 3, -4)$

(a) 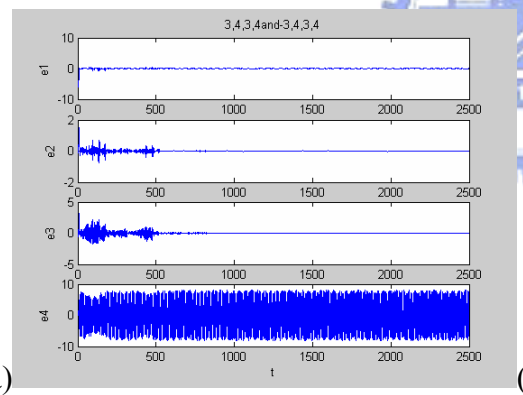

(b) 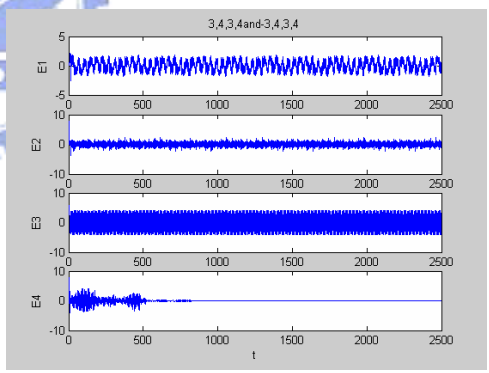

Fig. 3.8 CS and AS for initial condition$(x_2, y_2, u_2, v_2) = (-3, 4, 3, 4)$ and k=0.97,
(a) e_1, e_2, e_3, e_4 (b) E_1, E_2, E_3, E_4.

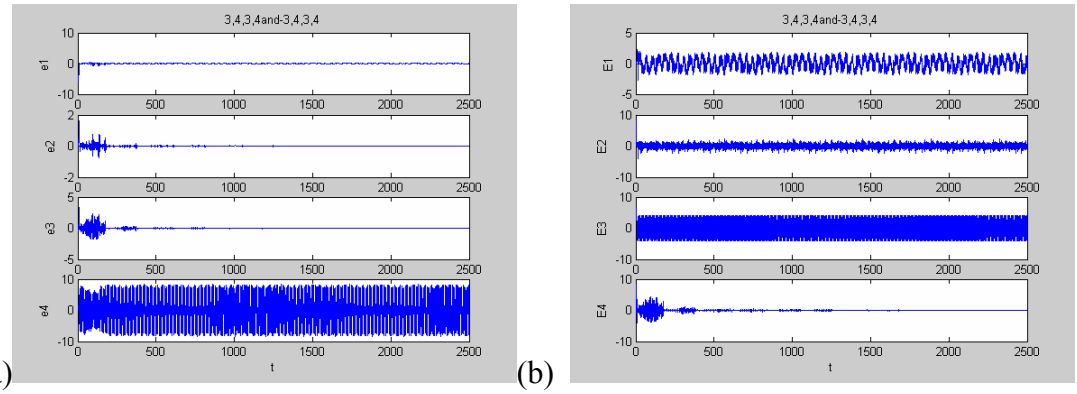

(a) (b)

Fig. 3.9 CS and AS for initial condition $(x_2, y_2, u_2, v_2) = (-3, 4, 3, 4)$ and k=1.02, (a) e_1, e_2, e_3, e_4 (b) E_1, E_2, E_3, E_4.

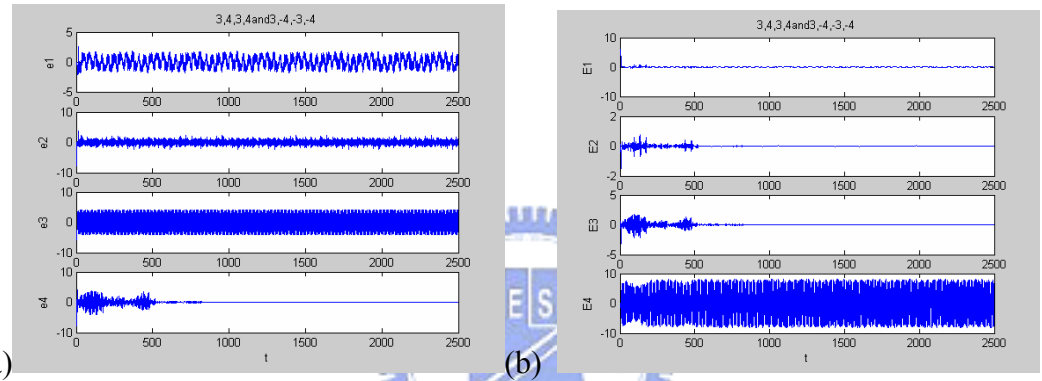

(a) (b)

Fig. 3.10 CS and AS for initial condition $(x_2, y_2, u_2, v_2) = (3, -4, -3, -4)$ and k=0.97, (a) e_1, e_2, e_3, e_4 (b) E_1, E_2, E_3, E_4.

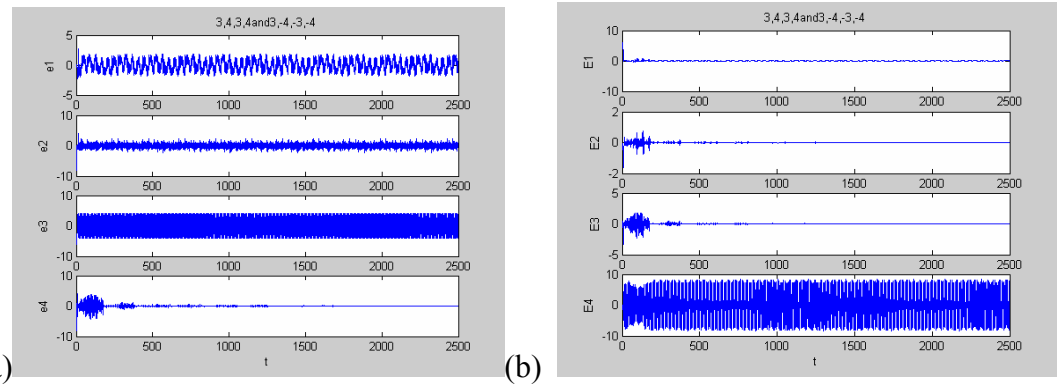

(a) (b)

Fig. 3.11 CS and AS for initial condition $(x_2, y_2, u_2, v_2) = (3, -4, -3, -4)$ and k=1.02, (a) e_1, e_2, e_3, e_4 (b) E_1, E_2, E_3, E_4.

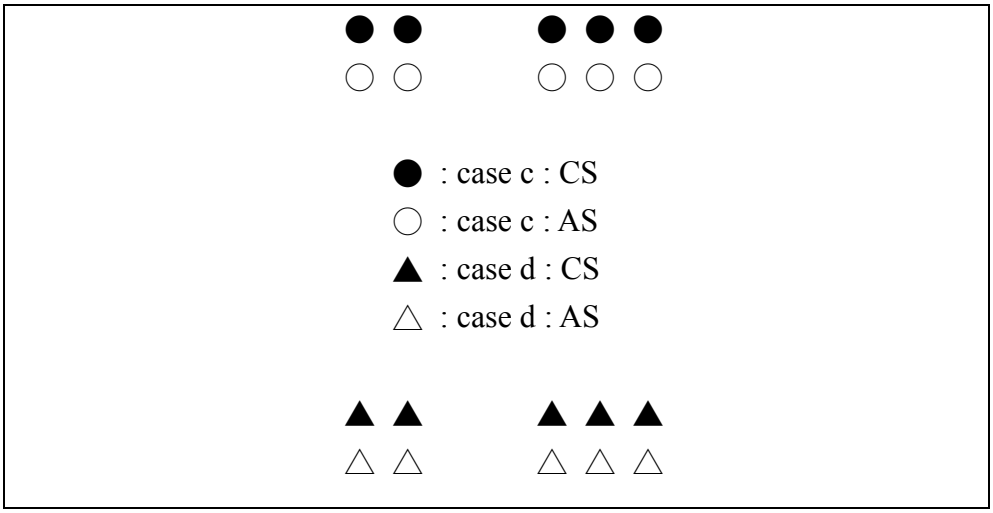

Fig. 3.12 CS or AS vs. the k for different initial conditions,

case c: $(x_1, y_1, u_1, v_1) = (3, 4, 3, 4)$ and $(x_2, y_2, u_2, v_2) = (-3, 4, 3, 4)$

case d: $(x_1, y_1, u_1, v_1) = (3, 4, 3, 4)$ and $(x_2, y_2, u_2, v_2) = (3, -4, -3, -4)$

Chapter 4

Uncoupled Chaos Synchronization and Antisynchronization of Double Van der Pol Systems by Noise Excited Parameters

4.1 Preliminaries

In this chapter, chaos complete synchronization and antisynchronization are obtained by replacing two corresponding parameters of two uncoupled identical double van der Pol chaotic dynamical systems by a white noise, or by a Rayleigh noise respectively.

4.2 Numerical simulations for uncoupled chaos synchronization and antisynchronization of double van der Pol systems by noise excited parameters

In this section, the double van der Pol system, studied in this chapter consists of two van der Pol systems with mutual coupling terms:

$$\begin{cases} \dfrac{dx_1}{dt} = y_1 \\ \dfrac{dy_1}{dt} = -x_1 + b(1 - cx_1^2)y_1 + au_1 \\ \dfrac{du_1}{dt} = v_1 \\ \dfrac{dv_1}{dt} = -u_1 + e(1 - fu_1^2)v_1 + dx_1 \end{cases} \tag{4.1}$$

where au_1, dx_1 are mutual coupling terms. When a = 0.04 , b = 0.2, c = 12 , d = -0.3, e = 2, f = 1, chaos of the system are illustrated by Lyapunov exponent diagram (Fig. 3.1) and phase portraits (Fig. 3.2).

Take system (4.1) as master system, the slave system is

$$\begin{cases} \dfrac{dx_2}{dt} = y_2 \\ \dfrac{dy_2}{dt} = -x_2 + b(1 - cx_2^{\,2})y_2 + au_2 \\ \dfrac{du_2}{dt} = v_2 \\ \dfrac{dv_2}{dt} = -u_2 + e(1 - fu_2^{\,2})v_2 + dx_2 \end{cases} \tag{4.2}$$

In order to obtain CS and AS of systems (4.1) and (4.2), the two corresponding parameters a of two systems are replaced respectively by a noise term $k\,f(x)$, where k is constant driving strength and $f(x)$ is a noise signal.

The error state variables are defined:

$$\begin{cases} e_1 = x_1 - x_2 \\ e_2 = y_1 - y_2 \\ e_3 = u_1 - u_2 \\ e_4 = v_1 - v_2 \end{cases} \tag{4.3}$$

Giving suitable values for k and initial conditions, CS or AS of systems (4.1) and (4.2) can be obtained.

Matlab method for simulations with time step 0.01. The parameters of systems (4.1) and (4.2) are given as a = 0.04, b = 0.2, c = 12 , d = -0.3, e = 2, f = 1 to ensure the chaotic behavior. To verify CS and AS, it is convenient to introduce the following coordinate transformation: $E_1 = (x_1 + x_2)$ and $e_1 = (x_1 - x_2)$ and the same transformation for *y, u* and v variables. Therefore, the new coordinate systems (E_1, E_2, E_3, E_4) and (e_1, e_2, e_3, e_4) represent the sum and difference motions of the original coordinate system, respectively. We can easily see that (e_1, e_2, e_3, e_4) subspace represents the CS case, and (E_1, E_2, E_3, E_4) subspace the AS one.

In order to obtain CS or AS of systems (4.1) and (4.2), we replace two

corresponding parameters a of two identical systems by the same noise signal as follow:

Case1: White noise

The probability density function of n-dimensional Gaussian noise is

$$f(x) = ((2\pi)^n \det K)^{-\frac{1}{2}} \exp(-(x-\mu)^T K^{-1}(x-\mu)/2)$$

where x is a length-one vector, K is the one-by-one covariance matrix, μ is the mean value vector, and the superscript T indicates matrix transpose. The Simulink Communications toolbox provides the Gaussian Noise Generator block. The initial seed, the mean value and the variance in the simulation must be specified. We take the initial seed 41, the mean value 1 and the variance 1 in the simulation.

Take $k\,f(x)$ instead of both a in system (4.1) and in system (4.2), and take $(x_1, y_1, u_1, v_1) = (3, 4, 3, 4)$, $(x_2, y_2, u_2, v_2) = (3, -4, 3, -4)$ as the initial conditions of system (4.1) and system (4.2). For Fig. 4.1, $k = 1$ and for Fig. 4.2, $k = 529$, simulation results indicate that parts of final states develops to CS or AS, depending on k for the identical initial conditions in both cases. In Fig. 4.1, e_1 (CS), e_2 (CS), e_3 (CS), E_4 (AS), converge to zero, while the other coordinates remain chaotic. In Fig. 4.2, on the other hand, e_4 (CS), E_1 (AS), E_2 (AS) ,E_3 (AS),converge to zero.

Depending on the initial conditions both AS and CS can also be observed. To study how these phenomena depend upon the initial conditions, we change the initial conditions for fixed k. The results are shown in Figs. 4.3 and 4.4. Fig. 4.3 (a) shows that only $e_4=v_1 - v_2$ tends to zero. In Fig. 4.3 (b), $E_1=x_1 + x_2$, $E_2=y_1 + y_2$, $E_3=u_1 + u_2$ tend to zero. One CS in Fig. 4.1 and three AS in Fig. 4.3, for different initial conditions complete all four states of the system. Similar result is obtained by comparing Fig. 4.2 with Fig. 4.4.

The simulation results are shown in Fig. 4.5 for different value of *k*. The solid circle "●" and triangle "▲" correspond to CS where parameter values *k* leads to synchronized behavior. While white circle "○" and triangle "△" indicate AS. It is discovered that system (4.1) and system (4.2) tend to either AS or CS by using combination of different *k* and initial values. However, as we can see from Fig. 4.5, both cases agree well with the fact that the system goes to either synchronized state or anti-synchronized state depending on initial values and on *k*. When *k* = -1 ~ 529, either synchronization or anti-synchronization is found.

Case2: Rayleigh noise

The Rayleigh probability density function is given by

$$f(x) = \begin{cases} \dfrac{x}{\sigma^2} e^{\frac{x^2}{2\sigma^2}} & x \geq 0 \\ 0 & x < 0 \end{cases}$$

where x is a length-one vector, σ^2 is known as the fading envelope of the Rayleigh distribution. The Simulink Communications toolbox provides the Rayleigh Noise Generator block. The initial seed and the sigma parameter in the simulation must be specified. We specify the initial seed 47 and the sigma parameter 5 in the simulation.

For this case, we take $k\, f(x)$ instead of both a in system (4.1) and system (4.2), and take $(x_1, y_1, u_1, v_1) = (3, 4, 3, 4)$, $(x_2, y_2, u_2, v_2) = (3, -4, 3, -4)$ as the initial conditions of system (4.1) and system (4.2). For Fig. 4.6, $k = 1$ and for Fig. 4.7, $k = 2379$, simulation results indicate that the final state develops to CS or AS, depending sensitively on *k*, while independent of the identical initial conditions. For Fig. 4.6, e_1 (CS) , e_2 (CS), e_3 (CS), E_4 (AS), converge to zero, while the other

coordinates remain chaotic. For the Fig. 4.7 , on the other hand, e_4 (CS) , E_1 (AS), E_2 (AS), E_3 (AS) converge to zero.

Depending on the initial conditions, both AS and CS can also be observed. To study how these phenomena depend upon the initial conditions, we change the initial conditions for fixed *k*. The results are shown in Figs. 4.8 and 4.9. Fig. 4.8 (a) shows that the difference $e_4=v_1 - v_2$ tends to zero. In Fig. 4.8 (b), the sums $E_1=x_1 + x_2$, $E_2=y_1 + y_2$, $E_3=u_1 + u_2$ tend to zero. Comparing Fig. 4.6 with Fig. 4.8 one can find that they have opposite behaviors. The only reason lies in the different initial conditions. Similar result is also obtained by comparing Fig. 4.7 with Fig. 4.9.

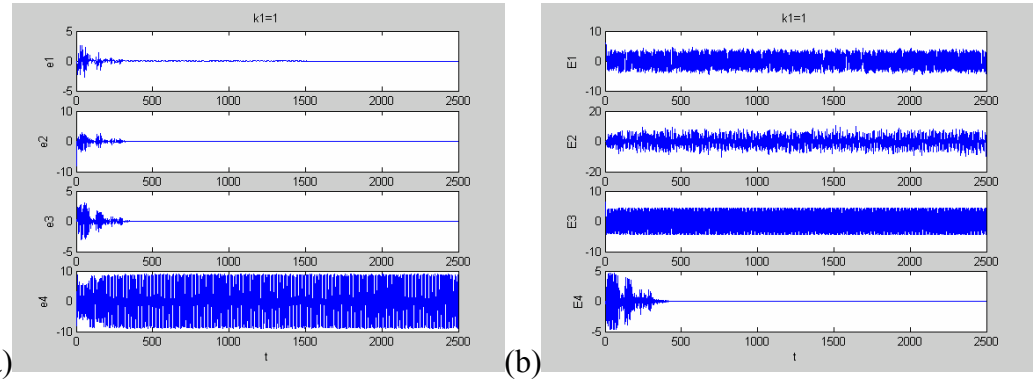

(a) (b)

Fig. 4.1 CS and AS for initial condition(x_2, y_2, u_2, v_2)= (3, -4, 3, -4) and k=1,

(a) e_1, e_2, e_3, e_4 (b) E_1, E_2, E_3, E_4

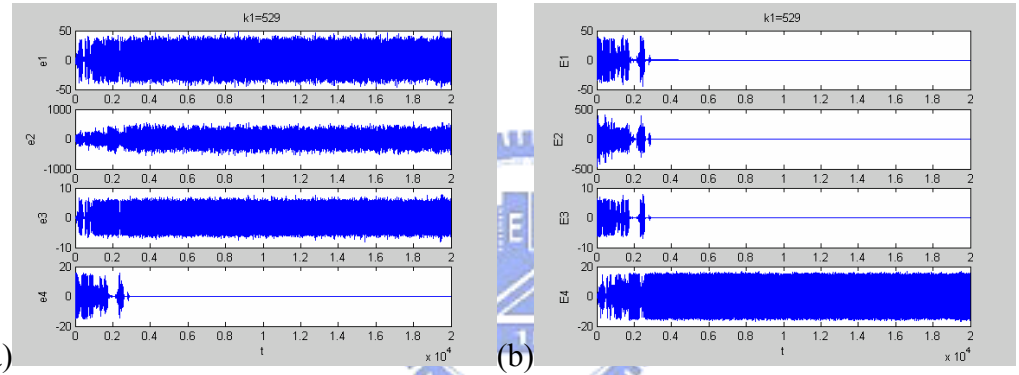

(a) (b)

Fig. 4.2 AS for initial condition (x_2, y_2, u_2, v_2) = (3, -4, 3, -4) and k=529,

(a)e_1, e_2, e_3, e_4 (b) E_1, E_2, E_3, E_4.

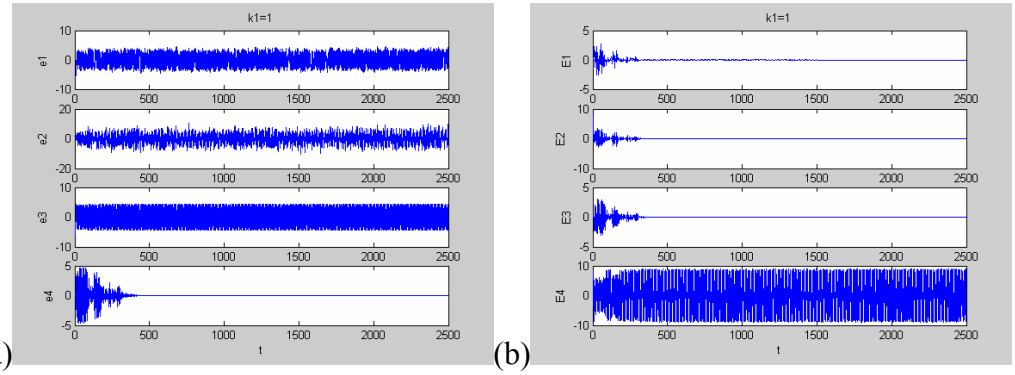

(a) (b)

Fig. 4.3 CS and AS for initial condition (x_2, y_2, u_2, v_2) = (-3, 4, -3, 4) and k=1,

(a) e_1, e_2, e_3, e_4 (b) E_1, E_2, E_3, E_4.

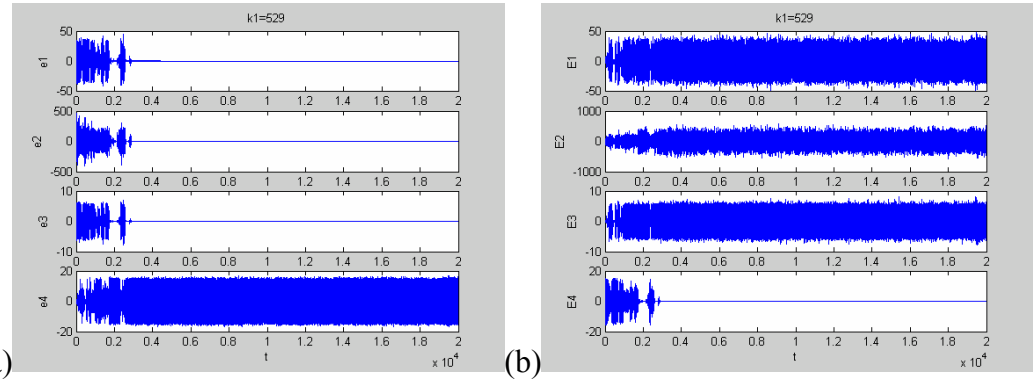

Fig. 4.4 CS for initial condition(x_2, y_2, u_2, v_2) = (-3, 4, -3, 4) and k=529,
(a) e_1, e_2, e_3, e_4 (b) E_1, E_2, E_3, E_4.

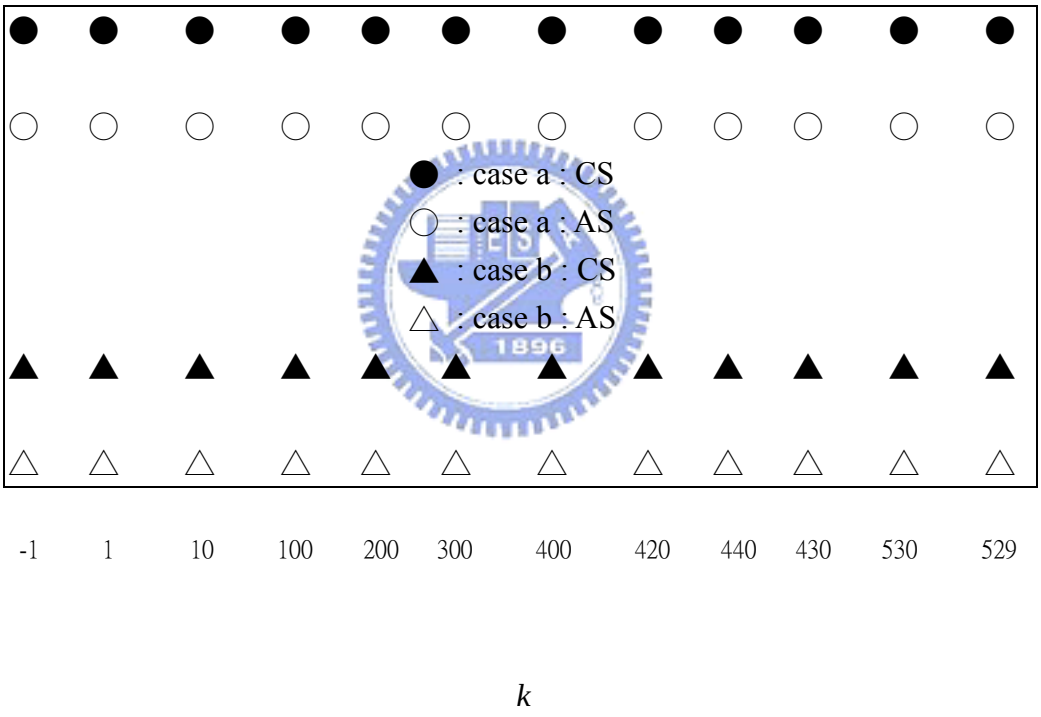

Fig. 4.5 CS or AS vs. the k for different initial conditions,
case a: (x_1, y_1, u_1, v_1) = (3, 4, 3, 4) and (x_2, y_2, u_2, v_2) = (3, -4, 3, -4)
case b: (x_1, y_1, u_1, v_1) = (3, 4, 3, 4) and (x_2, y_2, u_2, v_2) = (-3, 4, -3, 4)

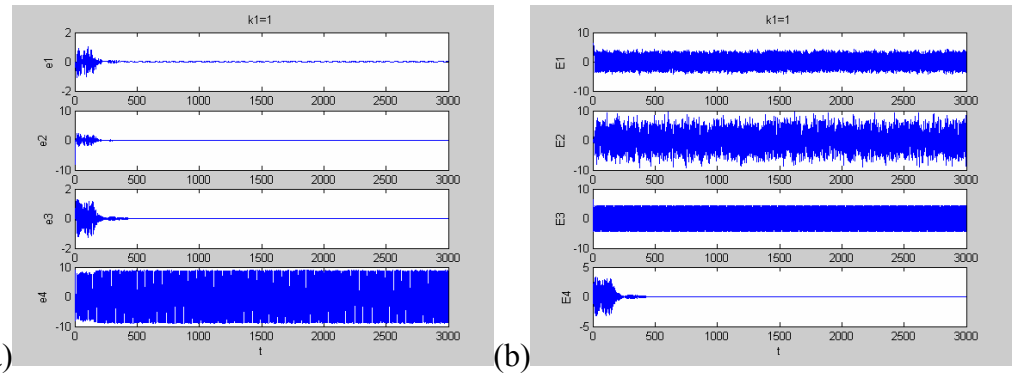

(a) (b)

Fig. 4.6 CS and AS for initial condition(x_2, y_2, u_2, v_2) = (3, -4, 3, -4) and k=1, (a) e_1, e_2, e_3, e_4 (b) E_1, E_2, E_3, E_4.

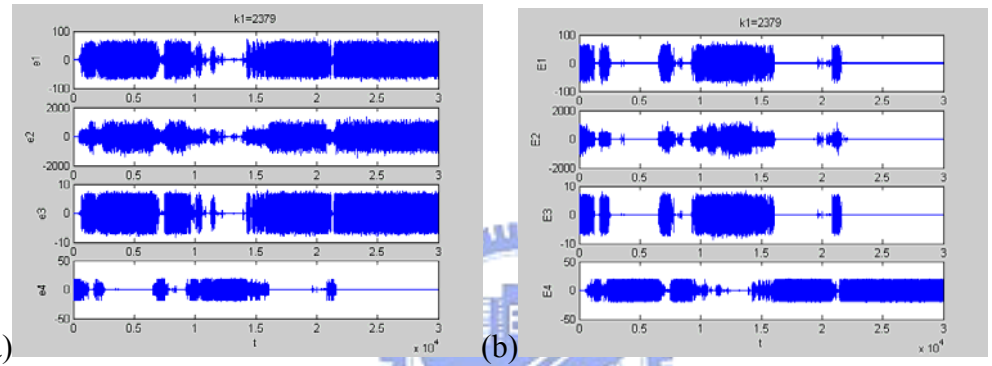

(a) (b)

Fig. 4.7 CS and AS for initial condition (x_2, y_2, u_2, v_2) = (3, -4, 3, -4) and k=2379, (a) e_1, e_2, e_3, e_4 (b) E_1, E_2, E_3, E_4.

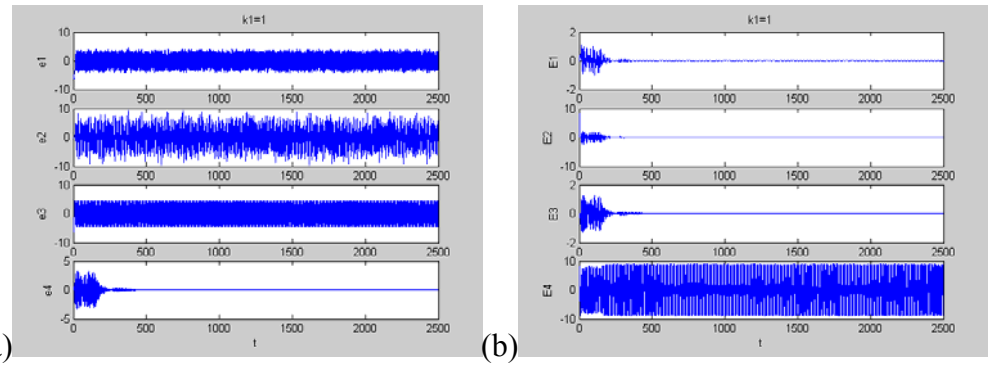

(a) (b)

Fig. 4.8 CS and AS for initial condition (x_2, y_2, u_2, v_2) = (-3, 4, -3, 4) and k=1 (a) e_1, e_2, e_3, e_4 (b) E_1, E_2, E_3, E_4.

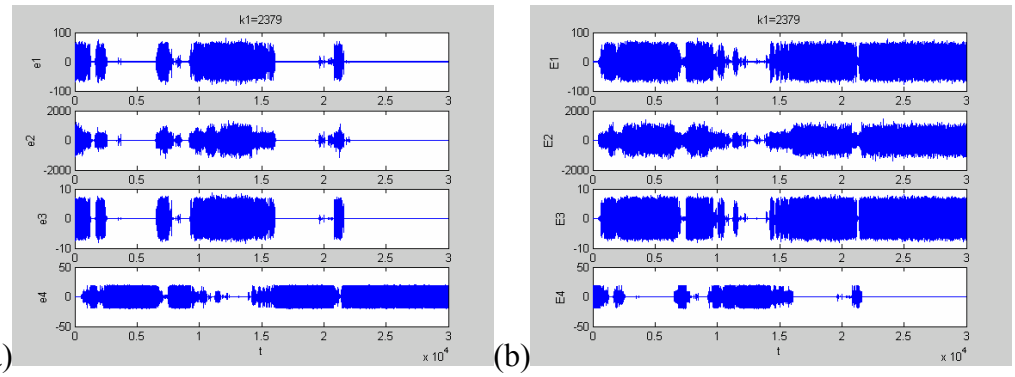

(a) (b)

Fig. 4.9 CS and AS for initial condition $(x_2, y_2, u_2, v_2) = (-3, 4, -3, 4)$ and k=2379, (a) e_1, e_2, e_3, e_4 (b) E_1, E_2, E_3, E_4.

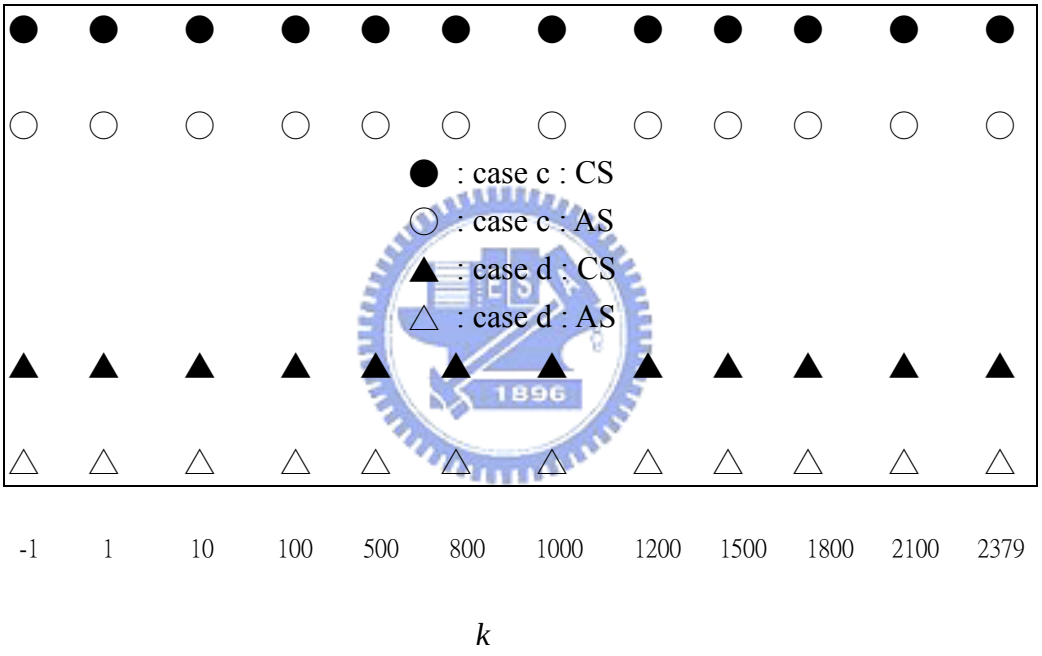

Fig. 4.10 CS or AS vs. the k for different initial conditions,
case c: $(x_1, y_1, u_1, v_1) = (3, 4, 3, 4)$ and $(x_2, y_2, u_2, v_2) = (3, -4, 3, -4)$
case d: $(x_1, y_1, u_1, v_1) = (3, 4, 3, 4)$ and $(x_2, y_2, u_2, v_2) = (-3, 4, -3, 4)$

Chapter 5

Pragmatical Adaptive Chaos Control from Double Van der Pol System to Double Duffing System

A new pragmatical adaptive control method for different chaotic systems is proposed. Traditional chaos control is limited for the same system. This method enlarges the function of chaos control. We can control a chaotic system, eg a double van der Pol system, to a given chaotic or regular system, eg a double Duffing system or an exponentially damoed-simple harmonic system. Based on a pragmatical theorem of asymptotical stability using the concept of probability, an adaptive control law is derived such that it can be proved strictly that the zero solution of error dynamics and of parameter dynamics is asymptotically stable.

5.1 Pragmatical adaptive control cheme

Consider the following chaotic system

$$\dot{x} = f(x, A) + u(t) \tag{5.1}$$

where $x = [x_1, x_2, \cdots, x_n]^T \in R^n$ denotes a state vector, $A = [A_1, A_2, ..., A_m] \in R^m$ is an original coefficient vector, and f is a vector function, and $u(t) = [u_1(t), u_2(t), \cdots, u_n(t)]^T \in R^n$ is a control input vector.

The goal system which can be either chaotic or nonchaotic, is

$$\dot{y} = g(y, \hat{B}) \tag{5.2}$$

where $y = [y_1, y_2, \cdots, y_n]^T \in R^n$ denotes a state vector, $\hat{B} = [\hat{B}_1, \hat{B}_2, ..., \hat{B}_p]^T \in R^p$ is a

goal coefficient vector, and g is a vector function. Our goal is to design an adaptive control method and a controller $u(t)$ so that the state vector of the chaotic system (5.1) asymptotically approaches the state vector of the goal system (5.2).

The chaos control is accomplished in the sense that the limit of the error vector $e(t) = [e_1, e_2, \cdots, e_n]^T$ approaches zero:

$$\lim_{t\to\infty} e = 0 \tag{5.3}$$

where

$$e = y - x \tag{5.4}$$

From Eq. (5.4) we have

$$\dot{e} = \dot{y} - \dot{x} \tag{5.5}$$

$$\dot{e} = g(y, \hat{B}) - f(x, A) - u(t) \tag{5.6}$$

A Lyapnuov function $V(e, \tilde{A}, \tilde{B})$ is chosen as a positive definite function

$$V(e, \tilde{A}, \tilde{B}) = \frac{1}{2} e^T e + \frac{1}{2} \tilde{A}^T \tilde{A} + \frac{1}{2} \tilde{B}^T \tilde{B} \tag{5.7}$$

where $\tilde{A} = A - \hat{A}$, $\tilde{B} = B - \hat{B}$, A and B are two column matrices whose elements are the original coefficients of systems (5.1) and (5.2) respectively, $\hat{A}, \hat{B}$ are two column matrices whose elements are the goal coefficients of systems (5.1) and (5.2) respectively.

Its derivative along any solution of the differential equation system consisting of Eq. (5.6) and update parameter differential equations for $\tilde{A}$ and $\tilde{B}$ is

$$\dot{V}(e) = e^T [g(y, \hat{B}) - f(x, A) - u(t)] + \tilde{A}\,\dot{\tilde{A}} + \tilde{B}\,\dot{\tilde{B}} \tag{5.8}$$

where $u(t)$, $\dot{\tilde{A}}$, and $\dot{\tilde{B}}$ are chosen so that $\dot{V} = e^T C e$, C is a diagonal negative definite matrix, and $\dot{V}$ is a negative semi-definite function of e and parameter differences $\tilde{A}$ and $\tilde{B}$. In current scheme of adaptive control of chaotic motion

[117-119], traditional asymptotical Lyapunov stability theorem and Babalat lemma are used to prove the error vector approaches zero, as time approaches infinity. But the question, why the estimated or given parameters also approach to the uncertain or goal parameters, remains no answer. By pragmatical asymptotical stability theorem, the question can be answered strictly.

The stability for many problems in real dynamical systems is actual asymptotical stability, although may not be mathematical asymptotical stability. The mathematical asymptotical stability demands that trajectories from all initial states in the neighborhood of zero solution must approach the origin as $t \to \infty$. If there are only a small part or even a few of the initial states from which the trajectories do not approach the origin as $t \to \infty$, the zero solution is not mathematically asymptotically stable. However, when the probability of occurrence of an event is zero, it means the event does not occur actually. If the probability of occurrence of the event that the trajectries from the initial states are that they do not approach zero when $t \to \infty$, is zero, the stability of zero solution is actual asymptotical stability though it is not mathematical asymptotical stability. In order to analyze the asymptotical stability of the equilibrium point of such systems, the pragmatical asymptotical stability theorem is used.

Let X and Y be two manifolds of dimensions m and n ($m<n$), respectively, and φ be a differentiable map from X to Y, then $\varphi(X)$ is subset of Lebesque measure 0 of Y [122]. For an autonomous system

$$\frac{dx}{dt} = f(x_1, \cdots, x_n) \tag{5.9}$$

where $x = [x_1, \cdots, x_n]^T$ is a state vector, the function $f = [f_1, \cdots, f_n]^T$ is defined on $D \subset R^n$ and $\|x\| \le H > 0$. Let x=0 be an equilibrium point for the system (5.9). Then

$$f(0) = 0 \tag{5.10}$$

Definition The equilibrium point for the system (5.9) is pragmatically asymptotically stable provided that with initial points on *C* which is a subset of Lebesque measure 0 of *D*, the behaviors of the corresponding trajectories cannot be determined, while with initial points on $D-C$, the corresponding trajectories behave as that agree with traditional asymptotical stability [120,121].

Theorem Let $V = [x_1, \cdots, x_n]^T : D \rightarrow R_+$ be positive definite and analytic on *D*, such that the derivative of *V* through Eq. (5.9), $\dot{V}$, is negative semi-definite.

Let *X* be the m-manifold consisted of point set for which $\forall x \neq 0$, $\dot{V}(x) = 0$ and *D* is a n-manifold. If $m+1<n$, then the equilibrium point of the system is pragmatically asymptotically stable.

Proof Since every point of *X* can be passed by a trajectory of Eq. (5.9), which is one- dimensional, the collection of these trajectories, *C*, is a $(m+1)$-manifold [123, 124].

If $m+1 < n$, then the collection *C* is a subset of Lebesque measure 0 of *D*. By the above definition, the equilibrium point of the system is pragmatically asymptotically stable.

If an initial point is ergodicly chosen in *D*, *the probability of that the initial point falls on the collection C is zero. Here, equal probability is assumed for every point chosen as an initial point in the neighborhood of the equilibrium point.* Hence, the event that the initial point is chosen from collection *C does not occur actually*. Therefore, under the equal probability assumption, pragmatical asymptotical stability becomes actual asymptotical stability. When the initial point falls on $D-C$, $\dot{V}(x) < 0$, the corresponding trajectories behave as that agree with

traditional asymptotical stability because by the existence and uniqueness of the solution of initial-value problem, these trajectories never meet *C*.

In Eq. (5.7) *V* is a positive definite function of *n* variables, i.e. *p* error state variables and *n*-*p*=*m* differences between unknown and estimated parameters, while $\dot{V} = e^T Ce$ is a negative semi-definite function of *n* variables. Since the number of error state variables is always more than one, *p*>1, *m*+1<*n* is always satisfied, by pragmatical asymptotical stability theorem we have

$$\lim_{t\to\infty} e = 0 \tag{5.11}$$

and the estimated parameters approach the uncertain parameters. The pragmatical adaptive control theorem is obtained. Therefore, the equilibrium point of the system is *pragmatically asymptotically stable. Under the equal probability assumption, it is actually asymptotically stable for both error state variables and parameter variables*.

5.2 Numerical results of the chaos ontrol

In this section, the double van der Pol system is:

$$\begin{cases} \dfrac{dx_1}{dt} = y_1 \\ \dfrac{dy_1}{dt} = a_1 x_1 + b_1 y_1 + c_1 x_1^2 y_1 + d_1 u_1 \\ \dfrac{du_1}{dt} = v_1 \\ \dfrac{dv_1}{dt} = j_1 x_1 + f_1 u_1 + g_1 v_1 + h_1 u_1^2 v_1 \end{cases} \tag{5.12}$$

where $d_1 u_1$, $j_1 x_1$ are mutual coupling terms. When a_1 = -1 , b_1 = 0.2, c_1 = -2.4 , d_1 = 0.04, j_1 = -0.3, f_1 = -1, g_1=2, h_1=-2 are original coefficients and initial

conditions are $x_1(0)=3$, $y_1(0)=4$, $u_1(0)=3$, and $v_1(0)=4$, chaos of the system are illustrated by phase portraits (Fig. 3.1).

Case (a) Control a chaotic double van der Pol system to a double Duffing system

The goal system is a double Duffing system. The Duffing system is

$$\ddot{x} + a\dot{x} + bx + cx^3 = d\cos\omega t \tag{5.13}$$

where a, b, c, d, ω are constant parameters, $d\cos\omega t$ is an external excitation. It can be written as two first order differential equations :

$$\begin{cases} \dfrac{dx}{dt} = y \\ \dfrac{dy}{dt} = -ay - bx - cx^3 + d\cos\omega t \end{cases} \tag{5.14}$$

Consider the following double Duffing system as goal system:

$$\begin{cases} \dfrac{dx_2}{dt} = y_2 \\ \dfrac{dy_2}{dt} = a_1 x_2 + \hat{b}_1 y_2 + \hat{c}_2 x_2^3 + \hat{d}_1 u_2 \\ \dfrac{du_2}{dt} = v_2 \\ \dfrac{dv_2}{dt} = \hat{j}_1 x_2 + f_1 u_2 + \hat{g}_1 v_2 + \hat{h}_2 u_2^3 \end{cases} \tag{5.15}$$

It consists of two Duffing systems in which two external excitations are replaced by two coupling terms. It is an autonomous system with four states where $\hat{b}_1$, $\hat{c}_2$, $\hat{d}_1$, $\hat{j}_1$, $\hat{g}_1$, and $\hat{h}_2$ are constant goal coefficients of the system. When $\hat{b}_1 = -0.05, \hat{c}_2 = -3, \hat{d}_1 = 7, \hat{j}_1 = -7, \hat{g}_1 = 0.05, \hat{h}_2 = -3$, the chaotic behavior is presented in Fig 5.1.

In order to lead (x_1, y_1, u_1, v_1) to (x_2, y_2, u_2, v_2), we add controllers U_1, U_2, U_3, and U_4 to each equation of Eq. (5.12), respectively.

$$\begin{cases} \dfrac{dx_1}{dt} = y_1 + U_1 \\ \dfrac{dy_1}{dt} = a_1 x_1 + b_1 y_1 + c_1 x_1^2 y_1 + d_1 u_1 + U_2 \\ \dfrac{du_1}{dt} = v_1 + U_3 \\ \dfrac{dv_1}{dt} = j_1 x_1 + f_1 u_1 + g_1 v_1 + h_1 u_1^2 v_1 + U_4 \end{cases} \tag{5.16}$$

We define error vector

$E = [E_1, E_2, E_3, E_4]^T = [x_2, y_2, u_2, v_2]^T - [x_1, y_1, u_1, v_1]^T$ .Subtracting Eq. (5.16) from Eq. (5.15), we obtain the error dynamics.

$$\begin{aligned} \dot{E}_1 &= y_2 - y_1 - U_1 \\ \dot{E}_2 &= a_1 x_2 + \hat{b}_1 y_2 + \hat{c}_2 x_2^3 + \hat{d}_1 u_2 - a_1 x_1 - b_1 y_1 - c_1 x_1^2 y_1 - d_1 u_1 - U_2 \\ \dot{E}_3 &= v_2 - v_1 - U_3 \\ \dot{E}_4 &= \hat{j}_1 x_2 + f_1 u_2 + \hat{g}_1 v_2 + \hat{h}_2 u_2^3 - j_1 x_1 - f_1 u_1 - g_1 v_1 - h_1 u_1^2 v_1 - U_4 \end{aligned} \tag{5.17}$$

where $E_1 = x_2 - x_1$, $E_2 = y_2 - y_1$, $E_3 = u_2 - u_1$, $E_4 = v_2 - v_1$.

Choose a Lyapunov function in the form of the positive definite function:

$$\begin{aligned} &V(E_1, E_2, E_3, E_4, \tilde{b}_1, \tilde{c}_1, \tilde{c}_2, \tilde{d}_1, \tilde{j}_1, \tilde{g}_1, \tilde{h}_1, \tilde{h}_2) \\ &= \frac{1}{2}(E_1^2 + E_2^2 + E_3^2 + E_4^2 + \tilde{b}_1^2 + \tilde{c}_1^2 + \tilde{c}_2^2 + \tilde{d}_1^2 + \tilde{j}_1^2 + \tilde{g}_1^2 + \tilde{h}_1^2 + \tilde{h}_2^2) \end{aligned} \tag{5.18}$$

where $\tilde{b}_1 = \hat{b}_1 - b_1$, $\tilde{c}_1 = \hat{c}_1 - c_1$, $\tilde{c}_2 = \hat{c}_2 - c_2$, $\tilde{d}_1 = \hat{d}_1 - d_1$, $\tilde{j}_1 = \hat{j}_1 - j_1$, $\tilde{g}_1 = \hat{g}_1 - g_1$, $\tilde{h}_1 = \hat{h}_1 - h_1$, $\tilde{h}_2 = \hat{h}_2 - h_2$ and $\hat{b}_1, \hat{c}_1, \hat{c}_2, \hat{d}_1, \hat{j}_1, \hat{g}_1, \hat{h}_1, \hat{h}_2,$ are goal parameters, $\hat{b}_1 = -0.05, \hat{c}_1 = 0, \hat{c}_2 = -3, \hat{d}_1 = 7, \hat{j}_1 = -7, \hat{g}_1 = 0.05, \hat{h}_1 = 0, \hat{h}_2 = -3$.

Its time derivative along any solution of Eq. (5.17) and parameter dynamics is

$$\begin{aligned}\dot{V} &= E_1[y_2 - y_1 - U_1] + E_2[a_1x_2 + \hat{b}_1y_2 + \hat{c}_2x_2^3 + \hat{d}_1u_2 - a_1x_1 - b_1y_1 - c_1x_1^2y_1 - d_1u_1 - U_2] \\ &+ E_3[v_2 - v_1 - U_3] + E_4[\hat{j}_1x_2 + f_1u_2 + \hat{g}_1v_2 + \hat{h}_2u_2^3 - j_1x_1 - f_1u_1 - g_1v_1 - h_1u_1^2v_1 - U_4] \\ &+ \tilde{b}_1(-\dot{b}_1) + \tilde{c}_1(-\dot{c}_1) + \tilde{c}_2(-\dot{c}_2) + \tilde{d}_1(-\dot{d}_1) \\ &+ \tilde{j}_1(-\dot{j}_1) + \tilde{g}_1(-\dot{g}_1) + \tilde{h}_1(-\dot{h}_1) + \tilde{h}_2(-\dot{h}_2)\end{aligned}$$

(5.19)

Choose

$$\begin{aligned}U_1 &= y_2 - y_1 + E_1 \\ U_2 &= a_1x_2 + \hat{b}_1y_2 + \hat{c}_2x_2^3 + \hat{d}_1u_2 - a_1x_1 - b_1y_1 - c_1x_1^2y_1 - d_1u_1 + E_2 + \tilde{a}_1^2 + \tilde{b}_1^2 + \tilde{c}_1^2 + \tilde{c}_2^2 + \tilde{d}_1^2 \\ U_3 &= v_2 - v_1 + E_3 \\ U_4 &= \hat{j}_1x_2 + f_1u_2 + \hat{g}_1v_2 + \hat{h}_2u_2^3 - j_1x_1 - f_1u_1 - g_1v_1 - h_1u_1^2v_1 + E_4 + \tilde{e}_1^2 + \tilde{f}_1^2 + \tilde{g}_1^2 + \tilde{h}_1^2 + \tilde{h}_2^2\end{aligned}$$

(5.20)

$$\begin{aligned}-\dot{b}_1 &= \tilde{b}_1E_2 \\ -\dot{c}_1 &= \tilde{c}_1E_2 \\ -\dot{c}_2 &= \tilde{c}_2E_2 \\ -\dot{d}_1 &= \tilde{d}_1E_2 \\ -\dot{j}_1 &= \tilde{j}_1E_4 \\ -\dot{g}_1 &= \tilde{g}_1E_4 \\ -\dot{h}_1 &= \tilde{h}_1E_4 \\ -\dot{h}_2 &= \tilde{h}_2E_4\end{aligned}$$

(5.21)

Eq.(5.21) is the parameter dynamics. Substituting Eq. (5.20) and Eq. (5.21) into Eq. (5.16), we obtain

$$\dot{V} = E_1^2 - E_2^2 - E_3^2 - E_4^2 < 0$$

which is a negative semi-definite function of E_1, E_2, E_3, E_4, $\tilde{b}_1, \tilde{c}_1, \tilde{c}_2, \tilde{d}_1, \tilde{e}_1, \tilde{g}_1, \tilde{h}_1, \tilde{h}_2,$. The Lyapunov asymptotical stability theorem is not satisfied. We cannot obtain that the common origin of error dynamics (5.17) and parameter dynamics (5.18) is asymptotically stable. Now, D is an 8-manifold, n=12 and the number of error state variables p=4. When E_1=E_2=E_3=E_4=0 and

$\tilde{b}_1, \tilde{c}_1, \tilde{c}_2, \tilde{d}_1, \tilde{e}_1, \tilde{g}_1, \tilde{h}_1, \tilde{h}_2$, take arbitrary values, $\dot{V} = 0$, so X is 4-manifold, $m=n-p=12-4=8$. $m+1<n$ is satisfied. By pragmatical asymptotical stability theorem, error vector e approaches zero and the estimated parameters also approach the uncertain parameters. The pragmatical generalized synchronization is obtained. Under the assumption of equal probability, it is actually asymptotically stable. This means that the chaos control for different systems, from a double van der Pol system to a double Duffing system, can be achieved. The simulation results are shown in Fig. 5.2 and Fig. 5.3.

Case (b) Control a chaotic double van der Pol system to a exponentially damped-simlpe harmonic system

Consider the following exponentially damped-simlpe harmonic system:

$$\begin{cases} \dfrac{dx_3}{dt} = -\hat{\lambda}_1 x_3 \\ \dfrac{dy_3}{dt} = -\hat{b}_1 y_3 \\ \dfrac{du_3}{dt} = v_3 \\ \dfrac{dv_3}{dt} = -\hat{f}_1 u_3 \end{cases} \tag{5.22}$$

In the first equation of Eq. (5.16), $k_1 = 1$.

$$\begin{cases} \dfrac{dx_1}{dt} = k_1 y_1 + U_1 \\ \dfrac{dy_1}{dt} = a_1 x_1 + b_1 y_1 + c_1 x_1^2 y_1 + d_1 u_1 + U_2 \\ \dfrac{du_1}{dt} = v_1 + U_3 \\ \dfrac{dv_1}{dt} = j_1 x_1 + f_1 u_1 + g_1 v_1 + h_1 u_1^2 v_1 + U_4 \end{cases} \tag{5.23}$$

where $k_1 = 1$, $a_1 = -1$, $b_1 = 0.2$, $c_1 = -2.4$, $d_1 = 0.04$, $j_1 = -0.3$, $f_1 = -1$, $g_1 = 2$,

h_1=-2, λ_1=0.

We define error vector

$E=[E_1, E_2, E_3, E_4]^T=[x_3, y_3, u_3, v_3]^T-[x_1, y_1, u_1, v_1]^T$ .Subtracting Eq. (5.23) from Eq. (5.22), we obtain the error dynamics.

$$\begin{aligned}
\dot{E}_1 &= -\hat{\lambda}_1 x_3 - k_1 y_1 - U_1 \\
\dot{E}_2 &= -\hat{b}_1 y_3 - a_1 x_1 - b_1 y_1 - c_1 x_1^2 y_1 - d_1 u_1 - U_2 \\
\dot{E}_3 &= v_3 - v_1 - U_3 \\
\dot{E}_4 &= -\hat{f}_1 u_3 - j_1 x_1 - f_1 u_1 - g_1 v_1 - h_1 u_1^2 v_1 - U_4
\end{aligned} \tag{5.24}$$

where $E_1=x_2-x_1$, $E_2=y_2-y_1$, $E_3=u_2-u_1$, $E_4=v_2-v_1$.

Choose a Lyapunov function in the form of the positive definite function:

$$\begin{aligned}
&V(E_1, E_2, E_3, E_4, \tilde{k}_1, \tilde{a}_1, \tilde{b}_1, \tilde{c}_1, \tilde{d}_1, \tilde{j}_1, \tilde{f}_1, \tilde{g}_1, \tilde{h}_1, \tilde{\lambda}_1) \\
&=\frac{1}{2}(E_1^2+E_2^2+E_3^2+E_4^2+\tilde{k}_1^2+\tilde{a}_1^2+\tilde{b}_1^2+\tilde{c}_1^2+\tilde{d}_1^2+\tilde{j}_1^2+\tilde{f}_1^2+\tilde{g}_1^2+\tilde{h}_1^2+\tilde{\lambda}_1^2)
\end{aligned} \tag{5.25}$$

where $\tilde{k}_1=\hat{k}_1-k_1$, $\tilde{a}_1=\hat{a}_1-a_1$, $\tilde{b}_1=\hat{b}_1-b_1$, $\tilde{c}_1=\hat{c}_1-c_1$, $\tilde{d}_1=\hat{d}_1-d_1$, $\tilde{j}_1=\hat{j}_1-j_1$, $\tilde{f}_1=\hat{f}_1-f_1$, $\tilde{g}_1=\hat{g}_1-g_1$, $\tilde{h}_1=\hat{h}_1-h_1$, $\tilde{\lambda}_1=\hat{\lambda}_1-\lambda_1$,

and $\hat{k}_1, \hat{a}_1, \hat{b}_1, \hat{c}_1, \hat{d}_1, \hat{j}_1, \hat{f}_1, \hat{g}_1, \hat{h}_1, \hat{\lambda}_1$, are goal parameters,

$\hat{k}_1=0, \hat{a}_1=0, \hat{b}_1=2, \hat{c}_1=0, \hat{d}_1=0, \hat{j}_1=0, \hat{f}_1=2.3, \hat{g}_1=0, \hat{h}_1=0, \hat{\lambda}_1=3$.

Its time derivative along any solution of Eq. (5.25) and parameter dynamics is

$$\begin{aligned}
\dot{V} &= E_1[-\hat{\lambda}_1 x_2 - k_1 y_1 - U_1] + E_2[-\hat{b}_1 y_3 - a_1 x_1 - b_1 y_1 - c_1 x_1^2 y_1 - d_1 u_1 - U_2] \\
&+ E_3[v_2 - v_1 - U_3] + E_4[-\hat{f}_1 u_3 - j_1 x_1 - f_1 u_1 - g_1 v_1 - h_1 u_1^2 v_1 - U_4] \\
&+ \tilde{k}_1(-\dot{k}_1) + \tilde{a}_1(-\dot{a}_1) + \tilde{b}_1(-\dot{b}_1) + \tilde{c}_1(-\dot{c}_1) + \tilde{d}_1(-\dot{d}_1) \\
&+ \tilde{j}_1(-\dot{j}_1) + \tilde{f}_1(-\dot{f}_1) + \tilde{g}_1(-\dot{g}_1) + \tilde{h}_1(-\dot{h}_1) + \tilde{\lambda}_1(-\dot{\lambda}_1)
\end{aligned} \tag{5.26}$$

Choose

$$
\begin{aligned}
U_1 &= -\hat{\lambda}_1 x_2 - k_1 y_1 + E_1 \\
U_2 &= -\hat{b}_1 y_3 - a_1 x_1 - b_1 y_1 - c_1 x_1^2 y_1 - d_1 u_1 + \tilde{a}_1^2 + \tilde{b}_1^2 + \tilde{c}_1^2 + \tilde{d}_1^2 + E_2 \\
U_3 &= E_3 \\
U_4 &= -\hat{f}_1 u_3 - j_1 x_1 - f_1 u_1 - g_1 v_1 - h_1 u_1^2 v_1 + \tilde{j}_1^2 + \tilde{f}_1^2 + \tilde{g}_1^2 + \tilde{h}_1^2 + E_4
\end{aligned}
\tag{5.27}
$$

$$
\begin{aligned}
-\dot{k}_1 &= \tilde{k}_1 E_1 \\
-\dot{a}_1 &= \tilde{a}_1 E_2 \\
-\dot{b}_1 &= \tilde{b}_1 E_2 \\
-\dot{c}_1 &= \tilde{c}_1 E_2 \\
-\dot{d}_1 &= \tilde{d}_1 E_2 \\
-\dot{j}_1 &= \tilde{j}_1 E_4 \\
-\dot{f}_1 &= \tilde{f}_1 E_4 \\
-\dot{g}_1 &= \tilde{g}_1 E_4 \\
-\dot{h}_1 &= \tilde{h}_1 E_4 \\
-\dot{\lambda}_1 &= \tilde{\lambda}_1 E_1
\end{aligned}
\tag{5.28}
$$

Eq.(5.28) is the parameter dynamics. Substituting Eq. (5.27) and Eq. (5.28) into Eq. (5.26), we obtain

$$\dot{V} = E_1^2 - E_2^2 - E_3^2 - E_4^2 < 0$$

which is a negative semi-definite function of E_1, E_2, E_3, E_4, $\tilde{k}_1, \tilde{a}_1, \tilde{b}_1, \tilde{c}_1, \tilde{d}_1, \tilde{j}_1, \tilde{f}_1, \tilde{g}_1, \tilde{h}_1, \tilde{\lambda}_1$, The Lyapunov asymptotical stability theorem is not satisfied. We cannot obtain that the common origin of error dynamics (5.24) and parameter dynamics (5.25) is asymptotically stable. Now, D is an 8-manifold, n=12 and the number of error state variables p=4. When E_1=E_2=E_3=E_4=0 and $\tilde{k}_1, \tilde{a}_1, \tilde{b}_1, \tilde{c}_1, \tilde{d}_1, \tilde{j}_1, \tilde{f}_1, \tilde{g}_1, \tilde{h}_1, \tilde{\lambda}_1$, take arbitrary values, $\dot{V} = 0$, so X is 4-manifold, m=n-p=12-4=8. m+1<n is satisfied. By pragmatical asymptotical stability theorem, error vector e approaches zero and the estimated parameters also approach the

uncertain parameters. The pragmatical generalized synchronization is obtained. Under the assumption of equal probability, it is actually asymptotically stable. This means that the chaos control for different systems, from a double van der Pol system to a exponentially damped-simlpe harmonic system, can be achieved. The simulation results are shown in Fig. 5.4 and Fig. 5.5.

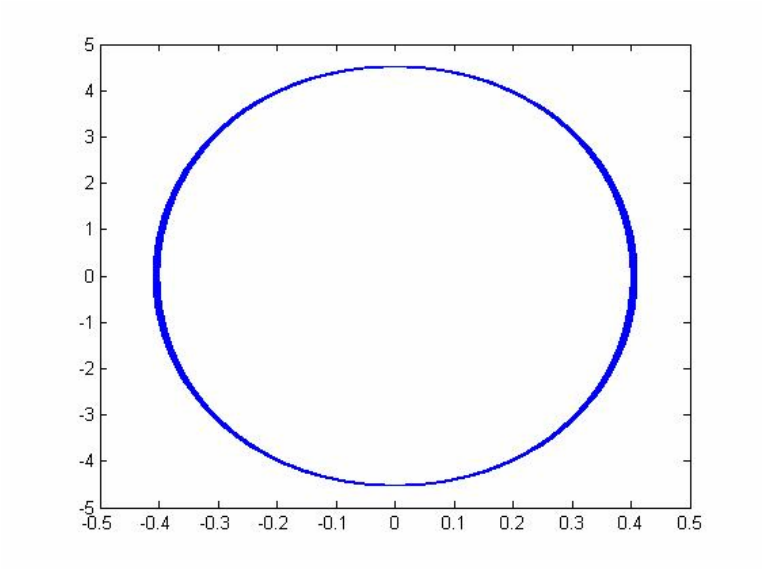

Fig. 5.1 Phase portraits of the double Duffing system

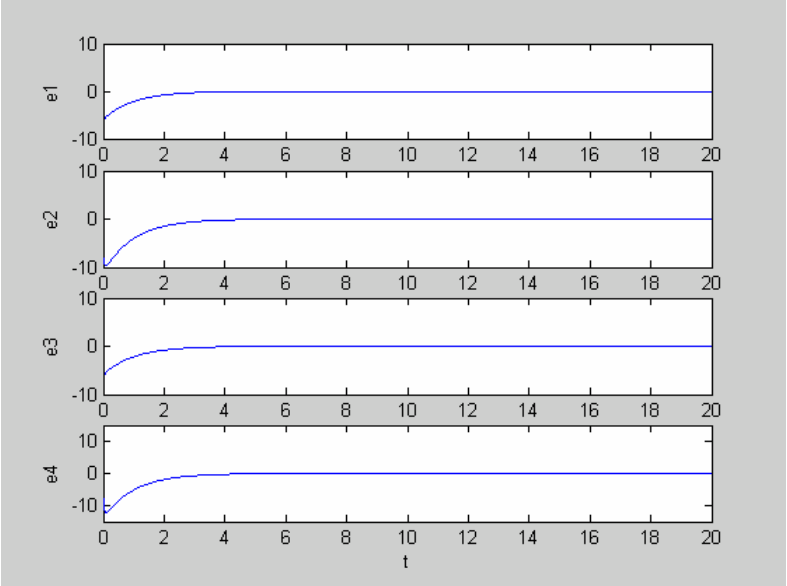

Fig. 5.2 Time histories of state errors for E_1, E_2, E_3, E_4 for Case (a)

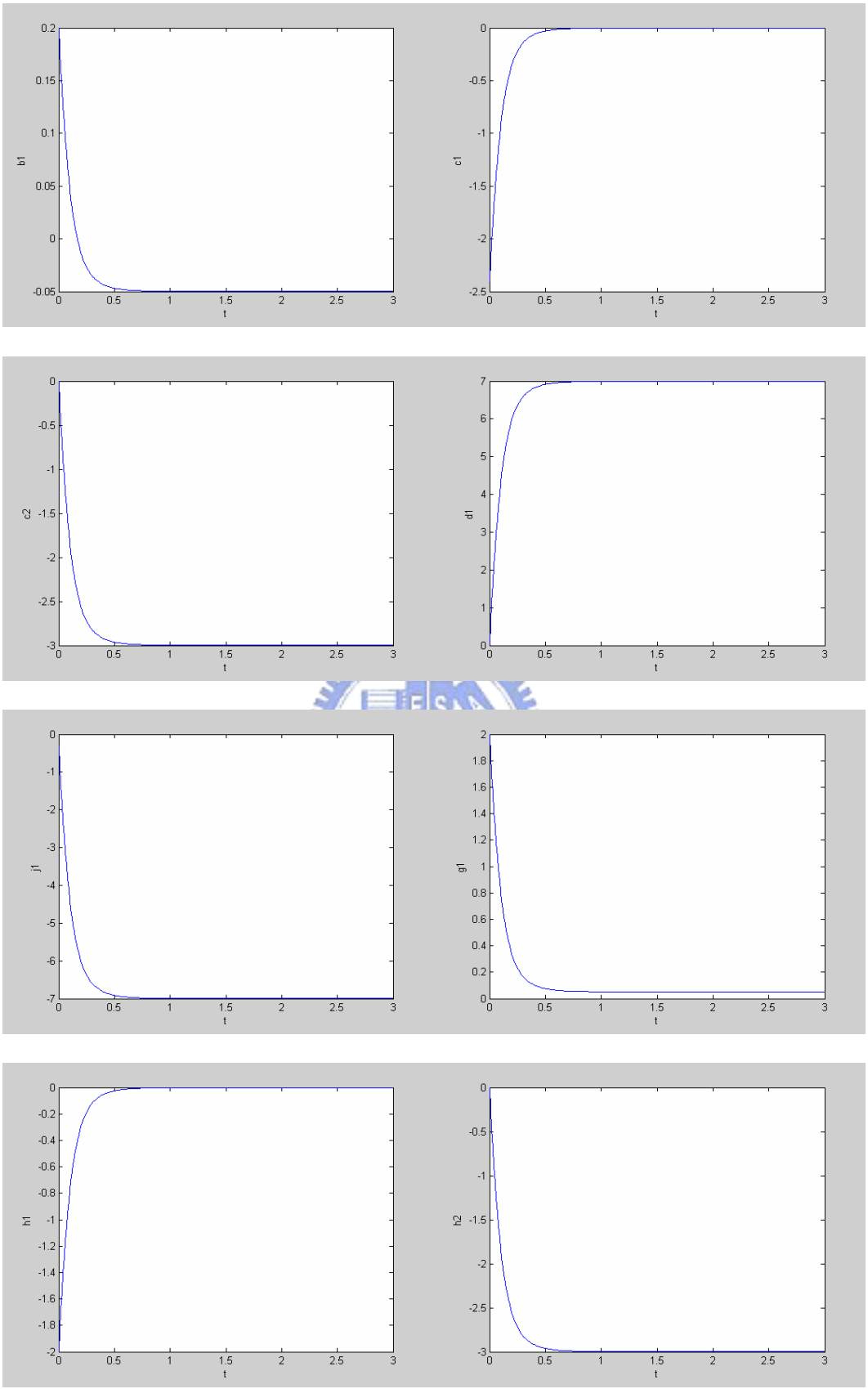

Fig. 5.3 Time histories of coefficients $b_1, c_1, c_2, d_1, j_1, g_1, h_1, h_2$ for Case (a)

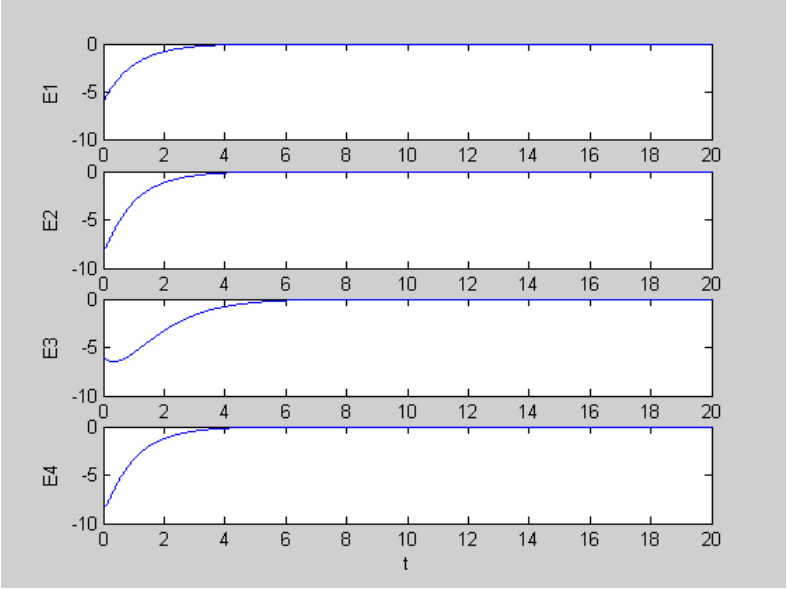

Fig. 5.4 Time histories of state errors for E_1, E_2, E_3, E_4 for Case (b)

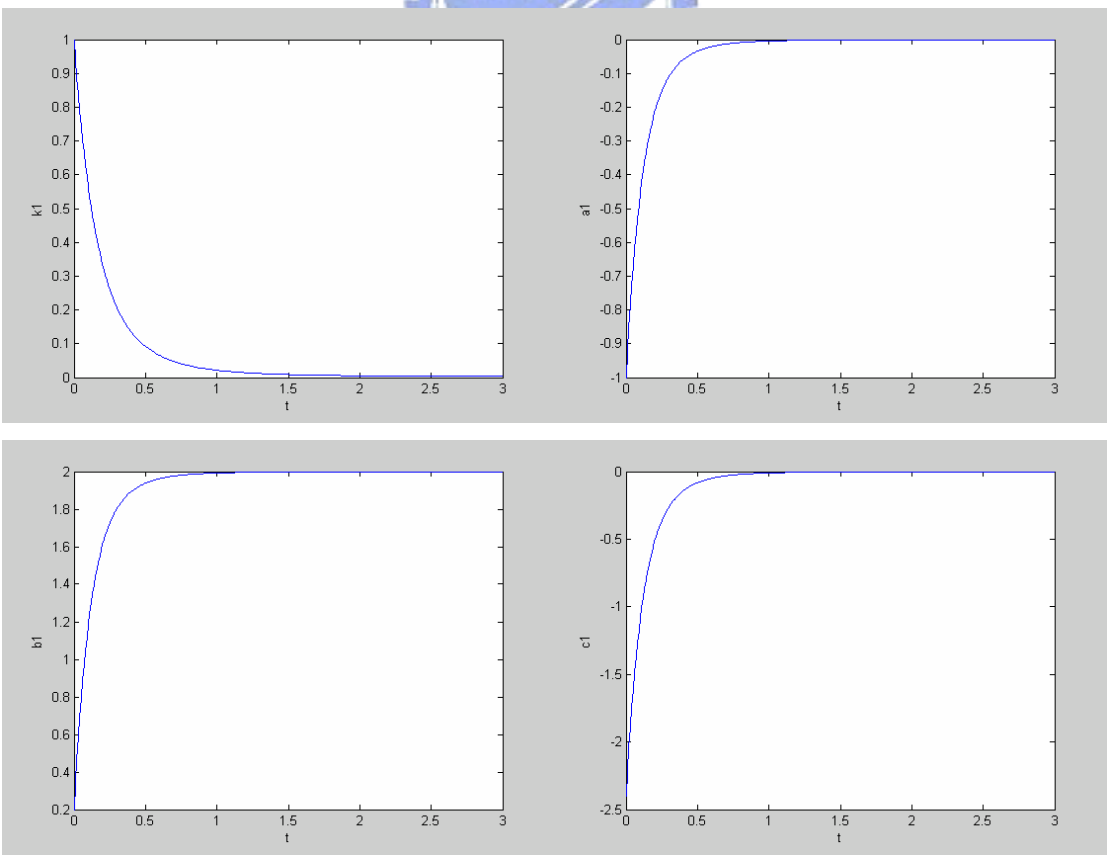

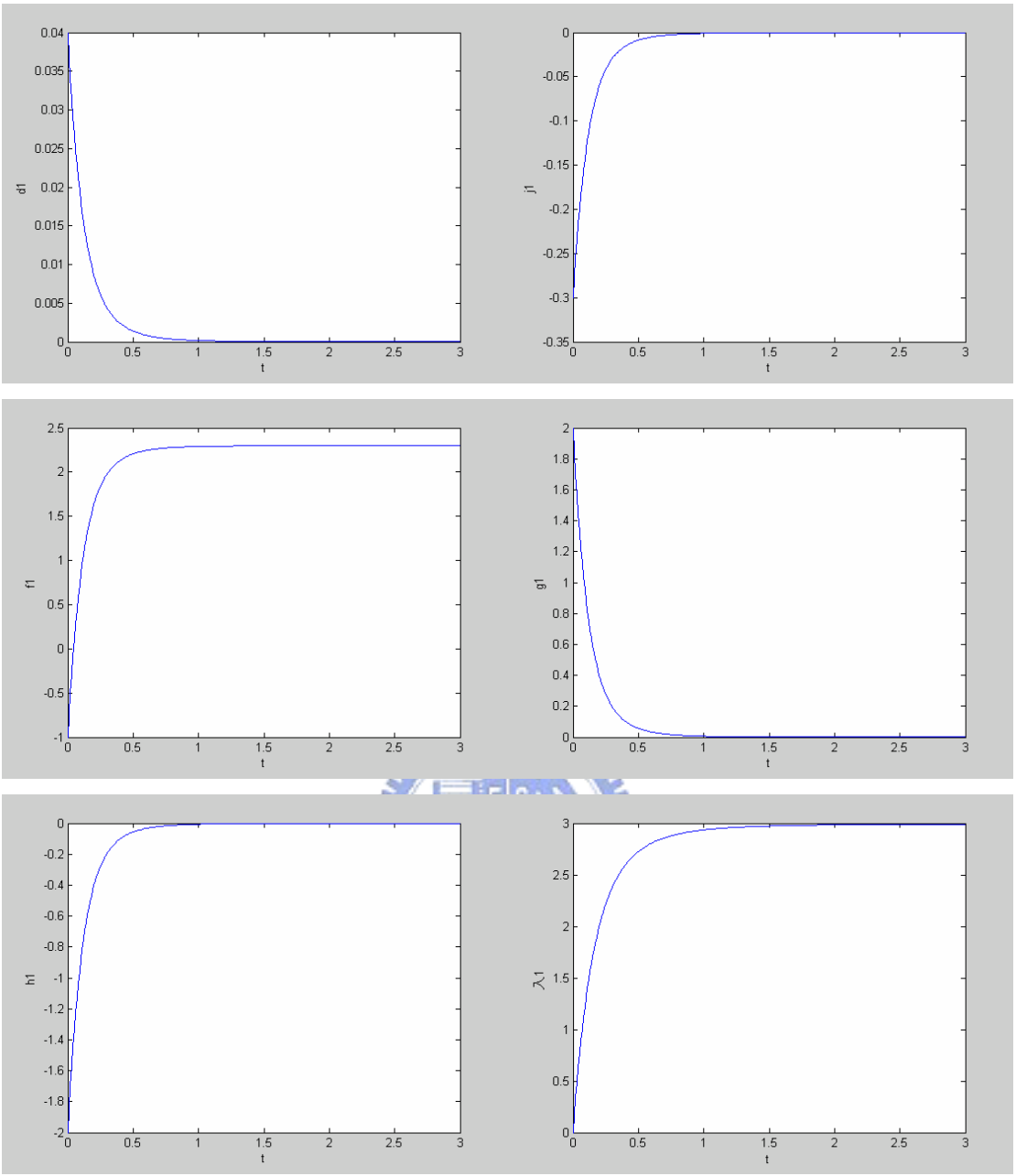

Fig. 5.5 Time histories of coefficients $k_1, a_1, b_1, c_1, d_1, j_1, f_1, g_1, h_1, \lambda_1$ for Case (b)

Chapter 6

Conclusions

In this thesis the chaos in double van der Pol system and in its fractional order systems is studied in Chapter 2. It is found that with reducing the total derivative order $\alpha_1+\beta_1+\alpha_2+\beta_2$ the ranges of the chaotic phase portraits of the system decrease and its shape changes differently for different choices of parameters.Twenty-one chaotic cases for $0.4\le(\alpha_1+\beta_1+\alpha_2+\beta_2)\le 4.0$ are studied, and the lowest total order for chaos existence in the system is found to be 0.4. Thirty nonchaotic cases are found.

In Chapter 3, the state variable with adjustable strength of a third double van der Pol system substituted for the strength of two corresponding mutual coupling terms of two uncoupled identical chaotic double van der Pol system, gives rise to their synchronization or anti-synchronization. Both CS and AS can be achived by adjusting the strength of the substituted state variable and the initial conditions.

In Chapter 4, complete synchronization and antisynchronization scheme based on the substitution of two corresponding parameters in two identical chaotic double van der Pol systems by a white noise, or by a Rayleigh noise respectively. For the white noise case and Rayleigh noise case, CS and AS are obtained for different noise strengths and initial conditions. Numerical simulations show that whether CS or AS occurs is sensitive to the noise strength.

In Chapter 5, to control chaotic systems to different systems is study by new pragmatical adaptive control method. The pragmatical asymptotical stability theorem fills the vacancy between the actual asymptotical stability and mathematical asymptotical stability, the conditions of the Lyapunov function for pragmatical asymptotical stability are lower than that for traditional asymptotical stability. By using this theorem, with the same conditions for Lyapunov function,

$V > 0$, $\dot{V} \leq 0$, as that in current scheme of adaptive chaos control, we not only obtain the adaptive control of chaotic systems but also prove that the estimated parameters approach the uncertain values. Traditional chaos control is limited for the same system. This method enlarges the function of chaos control. We can control a chaotic system to a given chaotic or nonchaotic system.

REFERENCES

[1] Ahmad W, Sprott JC "Chaos in fractional order system autonomous nonlinear systems", Chaos, Solitons & Fractals 16: 339-351, 2003.

[2] Oustaloup A., Levron F., Nanot F., Mathieu B. "Frequency band complex non integer differentiator: characterization and synthesis", IEEE Trans CAS-I 47: 25–40, 2000.

[3] Hartley T. T., Lorenzo C. F. "Dynamics and control of initialized fractional-order systems", Nonlinear Dyn 29: 201–33, 2002.

[4] Ahmad W., El-Khazali R., El-Wakil A. "Fractional-order Wien-bridge oscillator", Electr Lett 37: 1110–2, 2001.

[5] Li C., Liao X., Yu J. "Synchronization of fractional order chaotic systems", Phys Rev E 68: 067203, 2003.

[6] Arena P., Caponetto R., Fortuna L., Porto D. "Bifurcation and chaos in noninteger order cellular neural networks", Int J Bifur Chaos 7: 1527–39 1998.

[7] Arena P., Fortuna L., Porto D. "Chaotic behavior in noninteger-order cellular neural networks", Phys Rev E 61: 776–81.

[8] Arena P., Caponetto R., Fortuna L., Porto D. "Chaos in a fractional order Duffing system", In: Proc. ECCTD, Budapest 1259–62, 1997.

[9] Grigorenko I., Grigorenko E. "Chaotic dynamics of the fractional Lorenz system", Phys Rev Lett 91: 034101, 2003.

[10] Li C., Chen G. "Chaos and hyperchaos in fractional order Rössler equations", Physica A 341: 55-61, 2004.

[11] Ahmad W. M., Harb W. M. "On nonlinear control design for autonomous chaotic systems of integer and fractional orders", Chaos, Solitons & Fractals 18: 693–701, 2003.

[12] Wajdi M. Ahmad “Stabilization of generalized fractional order chaotic systems using state feedback control”, Chaos, Solitons and Fractals 22, 141-150, 2004.

[13] Li C., Chen G. “Chaos in the fractional order Chen system and its control”, Chaos, Solitons & Fractals 22, 549-554, 2004.

[14] Li C., Liao X., Yu J. “Synchronization of fractional order chaotic systems”, Phys Rev E 68: 067203, 2003.

[15] Delbosco D., Rodino L. “Existence and uniqueness for a nonlinear fractional differential equation”, J. Math. Anal. Appl. 204: 609–625, 1996.

[16] Diethelm K., Ford N.J. “Analysis of fractional differential equations”, J. Math. Anal. Appl. 265: 229–248, 2002.

[17] Podlubny I. *Fractional Differential Equations*, Academic Press, New York, 1999.

[18] Samko S., Kilbas A., Marichev O. *Fractional Integrals and Derivatives*, Gordon and Breach, Yverdon, 1993.

[19] Ge Zheng-Ming; Chen Chien-Cheng "Phase synchronization of coupled chaotic multiple time scales systems", Chaos, Solitons and Fractals 20: 639-647, 2004.

[20] Lin Wen-Hui; Zha, Ya-Pu "Nonlinear behavior for nanoscale electrostatic actuators with Casimir force", Chaos, Solitons and Fractals 23: 1777-1785, 2005.

[21] Krawiec Adam, Szydlowski Marek "Continuous pricing in oligopoly", Chaos, Solitons & Fractals 7: 2067-2073, 1996.

[22] Shen Jianwei, Xu Wei, Lei Youming "Smooth and non-smooth travelling waves in a nonlinearly dispersive Boussinesq equation", Chaos, Solitons and Fractals 23: 117-130, 2005.

[23] Ge Zheng-Ming, Chen Yen-Sheng "Synchronization of unidirectional coupled chaotic systems via partial stability", Chaos, Solitons and Fractals 21: 101-111,

2004.

[24] Ge Zheng-Ming, Chen Yen-Sheng "Adaptive synchronization of unidirectional and mutual coupled chaotic systems", Chaos, Solitons and Fractals 3: 881-888, 2005.

[25] Fang Hai-Ping, Hao Bai-Lin "Symbolic dynamics of the Lorenz equations", Chaos, Solitons & Fractals 7: 217-246, 1996.

[26] Aquino Gerardo, Grigolin, Paolo, Scafetta Nicola "Sporadic randomness, Maxwell's demon and the Poincaré recurrence times", Chaos, Solitons and Fractals 12: 2023-2038, 2001.

[27] Masoller C., Schifino A.C. Sicardi, Romanelli L. "Characterization of strange attractors of Lorenz model of general circulation of the atmosphere", Chaos, Solitons and Fractals 6: 357-366, 1995.

[28] Petrisor E., Misguich J.H., Constantinesc, D. "Reconnection in a global model of Poincaré map describing dynamics of magnetic field lines in a reversed shear tokamak", Chaos, Solitons and Fractals 5: 1085-1099,2003.

[29] Zheng-Ming Ge, Chan-Yi Ou "Chaos in a fractional order modified Duffing system", Chaos, Solitons and Fractals, in press.

[30] Zheng-Ming Ge, Chang-Xian Yi " Chaos in a nonlinear damped Mathieu System, in a nano Resonator system and in its fractional order systems", Solitons and Fractals, in press.

[31] Zheng-Ming Ge, Mao-Yuan Hsu " Chaos in a generalized van der Pol system and in its fractional order system", Chaos, Solitons and Fractals, in press.

[32] Zheng-Ming Ge, An-Ray Zhang "Chaos in a modified van der Pol system and in its fractional order systems", Chaos, Solitons and Fractals, in press.

[33] Tom T. Hartley, Carl F. Lorenzo, Helen Killory Qammer " Chaos in Fractional Order Chua's System", IEEE, Tran. on circuit and systems Vol 42, No 8, 1995.

[34] Pecora L.M., Carroll T.L., Synchronization in chaotic systems, *Phys Rev Lett*, Volume: 64, (1990), pp. 821--824

[35] Ge, Z.M., Yu, T.C., and Chen, Y.S., "Chaos synchronization of a horizontal platform system", Journal of Sound and Vibration 731-49, 2003.

[36] Ge, Z.M., Lin, T.N., "Chaos, chaos control and synchronization of electro-mechanical gyrostat system", Journal of Sound and Vibration Vol. 259; No.3, 2003.

[37] Ge, Z.M., Chen, Y.S., "Synchronization of unidirectional coupled chaotic systems via partial stability", Chaos, Solitons and Fractals Vol. 21; 101-11, 2004.

[38] Ge, Z.M., Chen, C.C., "Phase synchronization of coupled chaotic multiple time scales systems", Chaos, Solitons and Fractals Vol. 20; 639-47, 2004.

[39] Ge, Z.M., Lin, C.C. and Chen, Y.S., "Chaos, chaos control and synchronization of vibromrter system", Journal of Mechanical Engineering Science Vol. 218; 1001-20, 2004.

[40] Chen, H.K., Lin, T.N. and Chen, J.H., "The stability of chaos synchronization of the Japanese attractors and its application", Japanese Journal of Applied Physics Vol. 42; No. 12, 7603-10, 2003.

[41] Ge, Z.M. and Leu, W.Y., "Chaos synchronization and parameter identification for loudspeaker system" Chaos, Solitons and Fractals Vol. 21; 1231-47, 2004.

[42] Ge, Z.M. and Chang, C.M., "Chaos synchronization and parameter identification for single time scale brushless DC motor", Chaos, Solitons and Fractals Vol. 20; 889-903, 2004.

[43] Ge, Z.M. and Lee, J.K., "Chaos synchronization and parameter identification for gyroscope system", Applied Mathematics and Computation, Vol. 63; 667-82, 2004.

[44] Ge, Z.M. and Cheng, J.W., “Chaos synchronization and parameter identification of three time scales brushless DC motor”, Chaos, Solitons and Fractals Vol. 24; 597-616, 2005.

[45] Ge, Z.M. and Wu, H.W., “Chaos synchronization and chaos anticontrol of a suspended track with moving loads”, Journal of Sound and Vibration Vol. 270; 685-712, 2004.

[46] Ge, Z.M. and Yu, C.Y. and Chen, Y.S., “Chaos synchronization and chaos anticontrol of a rotational supported simple pendulum”, JSME International Journal, Series C,Vol. 47; No. 1, 233-41, 2004.

[47] Ge, Z.M., Cheng, J.W. and Chen ,Y.S., “Chaos anticontrol and synchronization of three time scales brushless DC motor system”, Chaos, Solitons and Fractals Vol. 22; 1165-82, 2004.

[48] Ge, Z.M. and Lee, C.I., “Anticontrol and synchronization of chaos for an autonomous rotational machine system with a hexagonal centrifugal governor”, Chaos, Solitons and Fractals Vol. 282; 635-48, 2005.

[49] Ge, Z.M. and Lee, C.I., “Control, anticontrol and synchronization of chaos for an autonomous rotational machine system with time-delay”, Chaos, Solitons and Fractals Vol. 23; 1855-64, 2005.

[50] Yang S.P., Niu H.Y., Tian G., et al. Synchronization chaos by driving parameter, Acta Phys. Sin., Volume: 50, (2001),pp.619--623

[51] Dai D., Ma X.K., Chaos synchronization by using intermittent parametric adaptive control method, *Phys. Lett. A*, Volume: 288, (2001), pp. 23--28

[52] Carroll, T.L., Heagy, J.F., Pecora, L.M., “Transforming signals with chaotic synchronization”, Phys. Rev. E;54:4676–80;1996.

[53] Kocarev, L., Parlitz, U., “Generalized synchronization, predictability, and equivalence of unidirectionally coupled dynamical systems”, Phys. Rev.

Lett.;76:1816–9;1996.

[54] Rosenblum, M.G., Pikovsky, A.S., Kurths J., “Phase synchronization of chaotic oscillators”, Phys. Rev. Lett.; 76:1804–7; 1996.

[55] Yang, S.S., Duan, C.K., “Generalized Synchronization in Chaotic Systems”, Chaos, Solitons and Fractals; 9:1703–7; 1998.

[56] Chen, G., Liu, S.T., “On generalized synchronization of spatial chaos”, Chaos, Solitons and Fractals; 15:311–8; 2003.

[57] Kim, C.M., Rim, S., Kye, W.H., Ryu, J.W., Park, Y.J., “Anti-synchronization of chaotic oscillators”, Phys. Lett. A;320:39–46;2003.

[58] Yang, S.P., Niu, H.Y., Tian, G., et al., “Synchronizing chaos by driving parameter”, Acta Phys. Sin.;50:619–23;2001.

[59] Dai, D., Ma, XK., “Chaos synchronization by using intermittent parametric adaptive control method”, Phys. Lett. A ;288:23–8; 2001.

[60] Chen, H.K. “Synchronization of two different chaotic systems: a new system and each of the dynamical systems Lorenz, Chen and Lü ”, Chaos, Solitons and Fractals Vol. 25; 1049-56, 2005.

[61] Chen, H.K., Lin, T.N., “Synchronization of chaotic symmetric gyros by one-way coupling conditions”, ImechE Part C: Journal of Mechanical Engineering Science Vol. 217; 331-40, 2003.

[62] Chen, H.K., “Chaos and chaos synchronization of a symmetric gyro with linear-plus-cubic damping”, Journal of Sound & Vibration, Vol. 255; 719-40, 2002.

[63] Ge, Z.M., Yu, T.C., and Chen, Y.S., “Chaos synchronization of a horizontal platform system”, Journal of Sound and Vibration 731-49, 2003.

[64] Ge, Z.M., Lin, T.N., “Chaos, chaos control and synchronization of electro-mechanical gyrostat system”, Journal of Sound and Vibration Vol. 259;

No.3, 2003.

[65] Ge, Z.M., Chen, Y.S., “Synchronization of unidirectional coupled chaotic systems via partial stability”, Chaos, Solitons and Fractals Vol. 21; 101-11, 2004.

[66] Ge, Z.M., Chen, C.C., “Phase synchronization of coupled chaotic multiple time scales systems”, Chaos, Solitons and Fractals Vol. 20; 639-47, 2004.

[67] Ge, Z.M., Lin, C.C. and Chen, Y.S., “Chaos, chaos control and synchronization of vibromrter system”, Journal of Mechanical Engineering Science Vol. 218; 1001-20, 2004.

[68] Chen, H.K., Lin, T.N. and Chen, J.H., “The stability of chaos synchronization of the Japanese attractors and its application”, Japanese Journal of Applied Physics Vol. 42; No. 12, 7603-10, 2003.

[69] Ge, Z.M. and Shiue, “Non-linear dynamics and control of chaos for Tachometer”, Journal of Sound and Vibration Vol. 253; No4, 2002.

[70] Ge, Z.M. and Lee, C.I.., “Non-linear dynamics and control of chaos for a rotational machine with a hexagonal centrifugal governor with a spring”, Journal of Sound and Vibration Vol. 262; 845-64, 2003.

[71] Ge, Z.M., Hsiao, C.M. and Chen, Y.S., “Non-linear dynamics and chaos control for a time delay Duffing system”, Int. J. of Nonlinear Sciences and Numerical Vol. 6; No. 2, 187-199, 2005.

[72] Ge, Z.M., Tzen, P.C. and Lee, S.C., “Parametric analysis and fractal-like basins of attraction by modified interpolates cell mapping”, Journal of Sound and Vibration Vol. 253; No. 3, 2002.

[73] Ge, Z.M. and Lee, S.C., “Parameter used and accuracies obtain in MICM global analyses”, Journal of Sound and Vibration Vol. 272; 1079-85, 2004.

[74] Ge, Z.M. and Leu, W.Y., “Chaos synchronization and parameter identification

for loudspeaker system" Chaos, Solitons and Fractals Vol. 21; 1231-47, 2004.

[75] Ge, Z.M. and Chang, C.M., "Chaos synchronization and parameter identification for single time scale brushless DC motor", Chaos, Solitons and Fractals Vol. 20; 889-903, 2004.

[76] Ge, Z.M. and Lee, J.K., "Chaos synchronization and parameter identification for gyroscope system", Applied Mathematics and Computation, Vol. 63; 667-82, 2004.

[77] Ge, Z.M. and Cheng, J.W., "Chaos synchronization and parameter identification of three time scales brushless DC motor", Chaos, Solitons and Fractals Vol. 24; 597-616, 2005.

[78] Ge, Z.M. and Chen, Y.S., "Adaptive synchronization of unidirectional and mutual coupled chaotic systems", Chaos, Solitons and Fractals Vol. 26; 881-88, 2005.

[79] Chen, H.K., "Global chaos synchronization of new chaotic systems via nonlinear control", Chaos, Solitons & Fractals 4; 1245-51, 2005.

[80] Chen, H.K. and Lee, C.I., "Anti-control of chaos in rigid body motion", Chaos, Solitons and Fractals Vol. 21; 957-965, 2004.

[81] Ge, Z.M. and Wu, H.W., "Chaos synchronization and chaos anticontrol of a suspended track with moving loads", Journal of Sound and Vibration Vol. 270; 685-712, 2004.

[82] Ge, Z.M. and Yu, C.Y. and Chen, Y.S., "Chaos synchronization and chaos anticontrol of a rotational supported simple pendulum", JSME International Journal, Series C,Vol. 47; No. 1, 233-41, 2004.

[83] Ge, Z.M. and Leu, W.Y., "Anti-control of chaos of two-degree-of-freedom louder speaker system and chaos system of different order system", Chaos, Solitons and Fractals Vol. 20; 503-21, 2004.

[84] Ge, Z.M., Cheng, J.W. and Chen ,Y.S., “Chaos anticontrol and synchronization of three time scales brushless DC motor system”, Chaos, Solitons and Fractals Vol. 22; 1165-82, 2004.

[85] Ge, Z.M. and Lee, C.I., “Anticontrol and synchronization of chaos for an autonomous rotational machine system with a hexagonal centrifugal governor”, Chaos, Solitons and Fractals Vol. 282; 635-48, 2005.

[86] Yinping Zhang and Jitao Sun, “Chaotic synchronization and anti-synchronization based on suitable separation”, Phys. Lett. A ;330:442–447; 2004.

[87] Jia Hu, Shihua Chen and Li Chen, “Adaptive control for anti-synchronization of Chua's chaotic system”, Phys. Lett. A ;339:455–460; 2005.

[88] Li Guo-Hui, “Synchronization and anti-synchronization of Colpitts oscillators using active control”, Chaos, Solitons and Fractals Vol. 26; 87-93, 2005.

[89] Guo-Hui Li and Shi-Ping Zhou, “An observer-based anti-synchronization”, Chaos, Solitons and Fractals Vol. 29; 495-498, 2006.

[90] Guo-Hui Li and Shi-Ping Zhou, “Anti-synchronization in different chaotic systems”, Chaos, Solitons and Fractals Vol. 32; 516-520, 2007.

[91] Qiankun Song and Jinde Cao, “Synchronization and anti-synchronization for chaotic systems”, Chaos, Solitons and Fractals Vol. 33; 929-939, 2007.

[92] Ge, Z.M. and Lee, C.I., “Control, anticontrol and synchronization of chaos for an autonomous rotational machine system with time-delay”, Chaos, Solitons and Fractals Vol. 23; 1855-64, 2005.

[93]Guy, Jumarie, “Fractional master equation: non-standard analysis and Liouville–Riemann derivative”. Chaos, Solitons and Fractals;12: 2577-87,2001.

[94] Sun, H.H., Abdelwahad A.A., Onaral B., IEEE Trans. Autom. Control;29: 441,1984.

[95] Ichise, M., Nagayanagi ,Y., Kojima, T., Electroanal J., Chem.;33:253,1971.

[96] Heaviside, O., Electromagnetic Theory, Chelsea, New York, 1971.

[97] Arena, P., Caponetto, R., Fortuna, L., Porto, D., "Bifurcation and chaos in noninteger order cellular neural networks". Int J Bifur Chaos;7:1527–39,1998.

[98] Arena, P., Fortuna, L., Porto, D., "Chaotic behavior in noninteger-order cellular neural networks". Phys Rev E ;61:776–81,2000.

[99] Ott E, Grebogi C, Yorke JA., ''Controlling chaos'', Phys Rev Lett, 64, pp.1196-9, 1990.

[100] Chen G, Dong X., *From chaos to order: methodologies, perspectives and applications*, Singapore: World Scientific; 1998.

[101] Chen G, Dong X. , ''On feedback control of chaotic continuous time systems'', IEEE Trans Circ Syst I, pp.591-601, 1993.

[102] Chen G, Yu X., ''On time-delayed feedback control of chaotic systems'', IEEE Trans Circ Syst I;46, pp.767-72, 1999.

[103] Guan X, Chen C, Fan Z, Peng H., ''Time-delay feedback control of time-delay chaotic systems'', Int J Bifurcat Chaos, pp.193-206, 2003.

[104] Keiji K, Michio H, Hideki K., ''Sliding mode control for a class of chaotic systems'', Phys Lett A, 245, pp.511-7, 1998.

[105] Jang M., ''Sliding mode control of chaos in the cubic Chua's circuit system'', Int J Bifurcat Chaos, 12, pp.1437-49, 2002.

[106] Fuh C, Tung P., ''Robust control for a class of nonlinear oscillators with chaotic attractors'', Phys Lett A, 218, pp.240-8, 1996.

[117] Yu X., ''Variable structure control approach for controlling chaos'', Chaos, Solitons and Fractals, 8, pp.1577-86, 1997.

[108] Yu Y, Zhang S., ''Controlling uncertain Lu system using backstepping design'', Chaos, Solitons and Fractals, 15, pp.897-902, 2003.

[109] Bernardo Mdi., ‘‘A purely adaptive controller to synchronize and control chaotic systems’’, Phys Lett A, 214, pp.139-44, 1996.

[110] Moez F. An adaptive feedback control of linearizable chaotic systems’’, Chaos, Solitons & Fractals, 15, pp.883-90, 2003.

[111] Cao YJ., ‘‘A nonlinear adaptive approach to controlling chaotic oscillators’’, Phys Lett A, 270, pp.171-6, 2000.

[112] Lu J, Chen G, Zhang S, Celikovsky S., ‘‘Bridge the gap between the Lorenz system and the Chen system’’, Int J Bifurcat Chaos, 12, pp.2917-26, 2002.

[113] Lu J, Chen G, Zhang S., ‘‘A new chaotic attractor coined’’, Int J Bifurcat Chaos, pp.659-61, 2002.

[114] Hua C, Long C, Guan X, Duan G., ‘‘Robust stabilization of uncertain dynamic time-delay systems with unknown bounds of uncertainties’’, American Control Conference, pp. 3365-3370, 2002.

[115] Ge, Zheng-Ming and Yi, Chang-Xian, “Chaos in a nonlinear damped Mathieu system, in a nano resonator system and in its fractional order systems”, Chaos, Solitons and Fractals, 32, pp.42-61, 2007.

[116] Luigi Fortuna & Domenico Porto, ‘‘Quantum-CNN to generate nanscale chaotic oscillator’’, International Journal of Bifurcation and Chaos, 14(3), pp. 1085–1089, 2004.

[117] Park Ju H., ‘‘Adaptive synchronization of hyperchaotic Chen system with uncertain parameters’’, Chaos, Solitons and Fractals, 26, pp. 959-964, 2005.

[118] Park Ju H., ‘‘Adaptive synchronization of Rossler system with uncertain parameters’’, Chaos, Solitons and Fractals, 25, pp. 333-338, 2005.

[119] Elabbasy, E. M., Agiza, H. N., and El-Desoky, M. M., ‘‘Adaptive synchronization of a hrperchaotic system with uncertain parameter’’, Chaos, Solitons and Fractals, 30, pp. 1133-1142, 2006.

[120] Ge, Z.-M., Yu, J.-K. and Chen, Y.-T., Chen, ‘‘Pragmatical asymptotical stability theorem with application to satellite system’’, Jpn. J. Appl. Phys., 38, pp. 6178-6179, 1999.

[121] Ge, Z.-M. and Yu, J.-K., ‘‘Pragmatical asymptotical stability theoremon partial region and for partial variable with applications to gyroscopic systems’’, The Chinses Journal of Mechanics, 16(4), pp. 179-187, 2000.

[122] Matsushima, Y., *Differentiable Manifolds*, Marcel Dekker, City, 1972.

[123] Ge, Z.-M. and Chang, C.-M., ”Chaos synchronization and parameters identification of single time scale brushless DC motors”, Chaos, Solitons and Fractals 20, pp. 883-903, 2004.

[124] Ge, Z.-M. and Chen, C.-C., ”Phase synchronization of coupled chaotic multiple time scales systems”, Chaos, Solitons and Fractals 20, pp. 639-647, 2004.

[125] Ge, Z.-M. and Leu, W.-Y., “Chaos synchronization and parameter identification for identical system”, Chaos, Solitons and Fractals, 21, pp.1231-1247, 2004.

[126] Ge, Z.-M. and Leu, W.-Y., “Anti-control of chaos of two-degrees-of- freedom louder speaker system and chaos synchronization of Different order systems”, Chaos, Solitons and Fractals 20, pp. 503-521, 2004.

[127] Ge, Z.-M. and Chen, Y.-S., “Synchronization of unidirectional coupled chaotic systems via partial stability”, Chaos, Solitons and Fractals, 21, pp.101-111, 2004.

[128] Ge, Z.-M. and Yang, C.-H., “Synchronization of complex chaotic systems in series expansion form,” accepted by Chaos, Solitons, and Fractals, 2006.

[129] Ge, Z.-M., Yang, C.-H., Chen, H.-H., and Lee, S.-C., “Non-linear dynamics and chaos control of a physical pendulum with vibrating and rotation support” , Journal of Sound and Vibration, 242 (2), pp.247-264, 2001.

[130] Van der Pol, B. “On relaxation oscillations”, Philosophical Magazine 2, 978-92, 1926.

[131] Van der Pol, B. and van der Mark, J. “Frequency demultiplication”, Nature 120, 363-4, 1927.

[132] Van der Pol, B. and van der Mark, J. “The heartbeat considered as a relaxation oscillation and an electrical model of the heart”, Philosophical Magazine 6, 763-75, 1928.

[133] Kim C.-M., Rim S., Kye W.-H., Ryu J.-W., Park Y.-J., Anti-synchronization of chaotic oscillators, *Phys. Lett. A*, Volume: 320, (2003), pp. 39--46

Appendix

Table 1. FRACTIONAL OPERATORS WITH APPROXIMATELY 2 db ERROR FROM $\omega = 10^{-2}$ TO 10^{2} rad/sec

$\frac{1}{s^{0.1}} \approx \frac{220.4s^4 + 5004s^3 + 503s^2 + 234.5s + 0.484}{s^5 + 359.8s^4 + 5742s^3 + 4247s^2 + 147.7s + 0.2099}$
$\frac{1}{s^{0.2}} \approx \frac{60.95s^4 + 816.9s^3 + 582.8s^2 + 23.24s + 0.04934}{s^5 + 134s^4 + 956.5s^3 + 383.5s^2 + 8.953s + 0.01821}$
$\frac{1}{s^{0.3}} \approx \frac{23.76s^4 + 224.9s^3 + 129.1s^2 + 4.733s + 0.01052}{s^5 + 64.51s^4 + 252.2s^3 + 63.61s^2 + 1.104s + 0.002267}$
$\frac{1}{s^{0.4}} \approx \frac{25s^4 + 558.5s^3 + 664.2s^2 + 44.15s + 0.1562}{s^5 + 125.6s^4 + 840.6s^3 + 317.2s^2 + 7.428s + 0.02343}$
$\frac{1}{s^{0.5}} \approx \frac{15.97s^4 + 593.2s^3 + 1080s^2 + 135.4s + 1}{s^5 + 134.3s^4 + 1072s^3 + 543.4s^2 + 20.1s + 0.1259}$
$\frac{1}{s^{0.6}} \approx \frac{8.579s^4 + 255.6s^3 + 405.3s^2 + 35.93s + 0.1696}{s^5 + 94.22s^4 + 472.9s^3 + 134.8s^2 + 2.639s + 0.009882}$
$\frac{1}{s^{0.7}} \approx \frac{4.406s^4 + 177.6s^3 + 209.6s^2 + 9.179s + 0.0145}{s^5 + 88.12s^4 + 279.2s^3 + 33.3s^2 + 1.927s + 0.0002276}$
$\frac{1}{s^{0.8}} \approx \frac{5.235s^3 + 1453s^2 + 5306s + 254.9}{s^4 + 658.1s^3 + 5700s^2 + 658.2s + 1}$
$\frac{1}{s^{0.9}} \approx \frac{1.766s^2 + 38.27s + 4.914}{s^3 + 36.15s^2 + 7.789s + 0.01}$